

# Search for sterile neutrinos by shower events at a future neutrino telescope

YABIN WANG AND OSAMU YASUDA

*Department of Physics, Tokyo Metropolitan University,  
Hachioji, Tokyo 192-0397, Japan*

## Abstract

It is pointed out that searching for sterile neutrinos at high energy regions at a future IceCube-like facility has advantages compared with that of reactor or short baseline accelerator neutrino experiments, in which the size of the detector and energy resolution make it difficult to gain good sensitivity for a large mass-squared difference. In this study we show that it is possible to improve constraints on sterile neutrino mixing  $\theta_{14}$  for  $1 \text{ eV}^2 \lesssim \Delta m_{41}^2 \lesssim 100 \text{ eV}^2$  by looking for a dip in the shower events at an IceCube-like neutrino telescope whose volume is at least 10 times as large as that of IceCube and duration is 10 years. We also give an analytic expression for the oscillation probabilities in two cases where the condition of one mass scale dominance is satisfied.

# 1 Introduction

Since Super-Kamiokande first gave firm evidence of neutrino oscillations in 1998, studying neutrino oscillations due to non-zero neutrino mass has become a promising direction of exploring new physics beyond the Standard Model of particle physics. According to LEP [1], there are only three light active neutrinos ( $\nu_e, \nu_\mu, \nu_\tau$ ). Based on atmospheric and solar neutrino experiments as well as reactor and accelerator experiments, there are three mass eigenstates ( $\nu_1, \nu_2, \nu_3$ ) with corresponding masses ( $m_1, m_2, m_3$ ). The three-flavor eigenstates of neutrinos are mixed with the three mass eigenstates via a  $3 \times 3$  unitary matrix, which is called the PMNS matrix. In the standard three-flavor framework of neutrino oscillations, there are six parameters: three mixing angles,  $\theta_{12}$ ,  $\theta_{13}$ , and  $\theta_{23}$ , two independent mass-squared differences  $\Delta m_{21}^2$  and  $\Delta m_{32}^2$ , where  $\Delta m_{ij}^2 = m_i^2 - m_j^2$  ( $i > j; i, j = 1, 2, 3$ ), and one CP phase,  $\delta$ . As for the problem of the neutrino mass hierarchy, if  $m_3 > m_2 > m_1$  we call it a normal ordering (NO), whereas, if  $m_3 < m_1 < m_2$ , it is called an inverted ordering (IO). Furthermore, based on atmospheric and solar neutrino experiments, there are two mass-squared differences:  $\Delta m_{\text{atm}}^2 \equiv |\Delta m_{32}^2| \simeq |\Delta m_{31}^2|$  and  $\Delta m_{\text{sol}}^2 \equiv \Delta m_{21}^2$ . Therefore, we have a hierarchy in the mass-squared differences:

$$|\Delta m_{31}^2| \simeq |\Delta m_{32}^2| \gg \Delta m_{21}^2. \quad (1)$$

The updated values of the above mentioned parameters are as follows [1]:

$$\sin^2 \theta_{12} = 0.307 \pm 0.013, \quad (2)$$

$$\sin^2 \theta_{13} = (2.18 \pm 0.07) \times 10^{-2}, \quad (3)$$

$$\sin^2 \theta_{23} = 0.545 \pm 0.021 \text{ (NO)}, \quad (4)$$

$$\sin^2 \theta_{23} = 0.547 \pm 0.021 \text{ (IO)}, \quad (5)$$

$$\Delta m_{21}^2 = (7.53 \pm 0.18) \times 10^{-5} \text{ eV}^2, \quad (6)$$

$$\Delta m_{32}^2 = (2.453 \pm 0.034) \times 10^{-3} \text{ eV}^2 \text{ (NO)}, \quad (7)$$

$$\Delta m_{32}^2 = (-2.546_{-0.040}^{+0.034}) \times 10^{-3} \text{ eV}^2 \text{ (IO)}, \quad (8)$$

$$\delta = 1.36 \pm 0.17 \pi \text{ rad}. \quad (9)$$

The first experimental anomaly that cannot be explained by the standard three-flavor scheme was given by LSND [2]. LSND was looking for an oscillation signal in the channel of  $\bar{\nu}_\mu \rightarrow \bar{\nu}_e$  and observed an excess of  $\bar{\nu}_e$  events above the background. This result was supported by the MiniBooNE experiment [3]. This anomaly can be solved if there is at least one extra neutrino, called a sterile neutrino (see, e.g., [4]), with a mass-squared difference of  $O(1) \text{ eV}^2$ , which is much larger than  $\Delta m_{\text{atm}}^2$  and  $\Delta m_{\text{sol}}^2$ .

Moreover, solar and reactor neutrino experiments showed that there are the so-called “gallium neutrino anomaly” [5] and “reactor antineutrino anomaly” [6, 7], in which the observed  $\nu_e$  and reactor  $\bar{\nu}_e$  event numbers are smaller than the theoretical prediction, and these anomalies may be solved by introducing the existence of light sterile neutrinos whose mass is in the order of 1 eV, which also motivates us to search for sterile neutrinos.<sup>1</sup>

---

<sup>1</sup>The result in Ref. [8] disfavors the new flux of reactor antineutrinos [6, 7], which provided the original motivation for reactor antineutrino anomaly from the shape analysis of the energy

While the combined results on the parameter space of  $(\sin^2 2\theta_{\mu e}, \Delta m_{41}^2)$ , where  $\sin^2 2\theta_{\mu e} = 4|U_{\mu 4}|^2|U_{e 4}|^2$ ,  $U_{e 4}$  and  $U_{\mu 4}$  are the elements of the PMNS matrix, given by DayaBay+Bugey-3 ( $\bar{\nu}_e \rightarrow \bar{\nu}_e$ ) and MINOS ( $\nu_\mu \rightarrow \nu_\mu$ ) [10] conflict with that of LSND, because of the uncertainty in the theoretical calculation of the reactor antineutrino flux [9], the constraint in the  $(\sin^2 2\theta_{\mu e}, \Delta m_{41}^2)$ -plane in Ref. [10] may not be as strong as they claimed. This encourages us to improve constraints on sterile neutrino mixing.

Observing high energy neutrinos at IceCube is advantageous to search for sterile neutrinos. Because of the matter effect, there can be a “dip” in the neutrino oscillation probability at certain neutrino energy for the disappearance channel of muon neutrinos.<sup>2</sup> By looking for the dip in the energy spectrum, we can constrain the upper and lower bounds of the mass-squared difference,  $\Delta m_{41}^2$ . Searching for sterile neutrinos at high energy regions at IceCube has advantages compared with that of lower energy experiments, such as reactor or short baseline accelerator neutrino experiments, in which the size of the detectors and energy resolution make it difficult to gain good sensitivity for a large mass-squared difference. In this article, we study the sensitivity to sterile neutrino oscillations using shower events at IceCube rather than track events studied in Ref. [14].

The rest of this article is organized as follows. In Section 2, we briefly introduce the (3+1)-scheme and IceCube experiment. In Section 3, we present some analytical formulae for oscillation probabilities. In Section 4, we perform a numerical analysis of shower events expected to be observed at a future IceCube-like facility. Finally, we draw our conclusions in Section 5. In Appendices A - E, we give some details of deriving analytical expressions of oscillation probabilities.

## 2 Preliminaries

### 2.1 (3+1)-scheme

The simplest extension of the standard three-flavor framework assumes that there is only one sterile neutrino. The mixing between neutrino flavor eigenstates ( $\nu_e, \nu_\mu, \nu_\tau, \nu_s$ ) and mass eigenstates ( $\nu_1, \nu_2, \nu_3, \nu_4$ ) is formulated as

$$\begin{pmatrix} \nu_e \\ \nu_\mu \\ \nu_\tau \\ \nu_s \end{pmatrix} = \begin{pmatrix} U_{e1} & U_{e2} & U_{e3} & U_{e4} \\ U_{\mu 1} & U_{\mu 2} & U_{\mu 3} & U_{\mu 4} \\ U_{\tau 1} & U_{\tau 2} & U_{\tau 3} & U_{\tau 4} \\ U_{s1} & U_{s2} & U_{s3} & U_{s4} \end{pmatrix} \begin{pmatrix} \nu_1 \\ \nu_2 \\ \nu_3 \\ \nu_4 \end{pmatrix}, \quad (10)$$

where  $\nu_s$  represents the flavor eigenstate of sterile neutrinos,  $\nu_4$  denotes the fourth mass eigenstate, and  $U_{\alpha i}$  ( $\alpha = e, \mu, \tau, s$ ;  $i = 1, 2, 3, 4$ ) denotes the element of the PMNS matrix  $U$ . As the (2+2)-scheme has been excluded by the atmospheric and solar neutrino data [15], we only consider the (3+1)-scheme in this study. In this scheme, the mass  $m_4$  of the fourth mass eigenstate is much larger than those of other

---

spectrum. However, as far as the overall normalization of reactor antineutrinos is concerned, there is uncertainty which is as large as that of the difference between the old and new flux [9] and it is not clear whether the reactor antineutrino anomaly is disfavored from the result of Ref. [8].

<sup>2</sup>See Refs. [11, 12, 13] for earlier references.

mass eigenstates. Therefore, we have

$$\Delta m_{41}^2 \simeq \Delta m_{42}^2 \simeq \Delta m_{43}^2 \gg |\Delta m_{31}^2| \simeq |\Delta m_{32}^2| \gg \Delta m_{21}^2. \quad (11)$$

Further, because the fourth mass eigenstate  $\nu_4$  is weekly mixed with the active three-flavor eigenstates ( $\nu_e, \nu_\mu, \nu_\tau$ ), we have the following constraint condition

$$|U_{\alpha 4}|^2 \ll 1 \quad (\alpha = e, \mu, \tau). \quad (12)$$

In this study, we adopt the following parametrization of  $U$ :

$$U = \mathcal{R}_{34}(\theta_{34}, \delta_3) \mathcal{R}_{24}(\theta_{24}, 0) \mathcal{R}_{14}(\theta_{14}, \delta_2) \mathcal{R}_{23}(\theta_{23}, 0) \mathcal{R}_{13}(\theta_{13}, \delta_1) \mathcal{R}_{12}(\theta_{12}, 0) \quad (13)$$

$$[\mathcal{R}_{ij}(\theta_{ij}, \delta_l)]_{pq} = \begin{cases} \cos \theta_{ij} & p = q = i, j \\ 1 & p = q \neq i, j \\ \sin \theta_{ij} e^{-i\delta_l} & p = i; q = j \\ -\sin \theta_{ij} e^{i\delta_l} & p = j; q = i \\ 0 & \text{otherwise.} \end{cases} \quad (14)$$

Propagation of the neutrino and anti-neutrino flavor eigenstates  $\Psi$  and  $\bar{\Psi}$  in matter can be described by

$$i \frac{d\Psi}{dt} = (U \mathcal{E} U^{-1} + \mathcal{A}) \Psi \quad (15)$$

$$i \frac{d\bar{\Psi}}{dt} = (U^* \mathcal{E} U^{*-1} + \bar{\mathcal{A}}) \bar{\Psi} \quad (16)$$

$$\Psi \equiv \begin{pmatrix} \nu_e \\ \nu_\mu \\ \nu_\tau \\ \nu_s \end{pmatrix}, \quad \bar{\Psi} \equiv \begin{pmatrix} \bar{\nu}_e \\ \bar{\nu}_\mu \\ \bar{\nu}_\tau \\ \bar{\nu}_s \end{pmatrix} \quad (17)$$

$$\mathcal{E} \equiv \text{diag}(0, \Delta E_{21}, \Delta E_{31}, \Delta E_{41}) \quad (18)$$

$$\begin{aligned} \mathcal{A} &\equiv \text{diag}(A_e - iB, -iB, -iB, -A_n) \\ &\equiv \text{diag}(A_e - iB, -iB, -iB, A_s) \end{aligned} \quad (19)$$

$$\begin{aligned} \bar{\mathcal{A}} &\equiv \text{diag}(-A_e - iB, -iB, -iB, A_n) \\ &\equiv \text{diag}(-A_e - iB, -iB, -iB, -A_s) \end{aligned} \quad (20)$$

$$A_e = \sqrt{2} G_F N_e = \left[ \frac{\rho}{2.6 \text{ (g} \cdot \text{cm}^{-3})} \right] \cdot \left( \frac{Y_e}{0.5} \right) \cdot 1.0 \times 10^{-13} \text{ eV} \quad (21)$$

$$A_s \equiv -A_n = \frac{1}{\sqrt{2}} G_F N_n \quad (22)$$

$$B = \frac{1}{2} \sigma_{tot} (N_p + N_n), \quad (23)$$

where  $\Delta E_{jk} \equiv \Delta m_{jk}^2 / (2E)$ ,  $E$  represents the energy of neutrinos,  $A_e$  represents the matter effect induced by the charged current (CC) interaction between  $\nu_e$  and electrons, and  $A_n \equiv -A_s$  represents the matter effect induced by the neutral current (NC) interaction of  $\nu_\alpha$  ( $\alpha = e, \mu, \tau$ ) with electrons,  $u$  and  $d$  quarks. Note that a  $4 \times 4$  matrix  $(E_1 + A_n) \mathbf{1}_4$  ( $(E_1 - A_n) \mathbf{1}_4$ ), which is proportional to the  $4 \times 4$  identity matrix  $\mathbf{1}_4$ , was subtracted from the right hand side of Eq. (15) (Eq. (16)), because it affects only the phase of the probability amplitude  $A(\nu_\alpha \rightarrow \nu_\beta)$  ( $A(\bar{\nu}_\alpha \rightarrow \bar{\nu}_\beta)$ )

and does not affect the oscillation probability  $P(\nu_\alpha \rightarrow \nu_\beta)$  ( $P(\bar{\nu}_\alpha \rightarrow \bar{\nu}_\beta)$ ).  $G_F = 1.17 \times 10^{-5} \text{ GeV}^{-2}$  is the Fermi constant,  $N_e$  is the number of electrons in the Earth per unit volume, which is approximately equal to the number  $N_n$  of neutrons in matter per unit volume,  $\rho$  is the density of matter, and  $Y_e = N_p/(N_p + N_n)$  is the relative number density of electrons in matter, where  $N_p$ , which is equal to  $N_e$  because an atom is electrically neutral, represents the number of protons per unit volume.  $B$  represents the absorption effect [16] and is related by the total neutrino–nucleon cross section  $\sigma_{tot}$  by Eq. (23), which leads to the expected result  $P(\nu_\alpha \rightarrow \nu_\alpha) = \exp[-\sigma_{tot}(N_p + N_n)L]$  in the absence of neutrino mixing.

In vacuum, if we adopt the condition of “one mass scale dominance”, which represents the case where only the terms including  $\Delta m_{41}^2$  dominate in the oscillation probability, we have the following formula of oscillation probability:

$$P(\nu_\alpha \rightarrow \nu_\beta) \simeq P(\bar{\nu}_\alpha \rightarrow \bar{\nu}_\beta) \simeq \left| \delta_{\alpha\beta} - \sin^2 2\theta_{\alpha\beta} \sin^2 \left( \frac{\Delta m_{41}^2 L}{4E} \right) \right|, \quad (24)$$

where

$$\sin^2 2\theta_{\alpha\beta} = 4|U_{\alpha 4}|^2 |\delta_{\alpha\beta} - |U_{\beta 4}|^2| \quad (\alpha, \beta = e, \mu, \tau, s), \quad (25)$$

and  $L$  represents the baseline length.

In the discussions on neutrino oscillations at high energy ( $E_\nu \gtrsim 1 \text{ TeV}$ ) with the baseline length of  $O(10^4) \text{ km}$ ,  $|\Delta m_{\text{atm}}^2 L/E|$  and  $|\Delta m_{\text{sol}}^2 L/E|$  are negligible, and the condition of the one mass scale dominance is satisfied. As we will see below, the effect of CP violation is negligible in this case. In the analytical treatment in Section 3, we discuss oscillation probability in the limit of one mass scale dominance.

## 2.2 IceCube experiment

IceCube is a neutrino observatory located at the South Pole. IceCube observes atmospheric and astrophysical neutrinos, whose energy ranges approximately from 100 GeV to above  $10^9 \text{ GeV}$ . Among the neutrino events, there are track and shower events. Track events are recorded by the Cherenkov light of muons produced by the CC interaction between muon neutrinos and nuclei in ice. Shower events include electromagnetic and hadronic shower events, which are produced by the CC interactions of  $\nu_e$  and  $\nu_\tau$  as well as the NC interactions of any flavor of neutrinos. Track events have good angular resolution but poor energy resolution, whereas shower events have poor angular resolution but good energy resolution.

When up-going neutrinos arrive at IceCube after passing through the Earth, the effective mixing angle in matter can be enhanced due to the matter effect and a dip can appear in the neutrino oscillation probability for the disappearance channel. By searching for the dip in the oscillation probability, we can give the lower and upper bounds on the third mass-squared difference  $\Delta m_{41}^2$ . This was done for the disappearance channel of muon neutrinos [14].

At high energy ( $\gtrsim 10 \text{ GeV}$ ) muon neutrinos constitute most atmospheric neutrinos because most high energy atmospheric muons do not decay into electrons and neutrinos before they reach the Earth. Therefore, at high energy the flux of atmospheric  $\nu_e + \bar{\nu}_e$ , which mainly come from kaon decays, is much smaller than that of

$\nu_\mu + \bar{\nu}_\mu$ . Despite this fact, motivated by the reactor antineutrino and gallium neutrino anomalies, we study the sensitivity of shower events to neutrino oscillations, anticipating the large detector volume may improve this disadvantage in the future.

In the energy range of 1-100 TeV, prompt neutrinos, which come from the decay of charmed mesons, may have fluxes of  $\nu_\mu$  and  $\nu_e$ , comparable to that of the conventional atmospheric neutrinos. Although prompt neutrinos can be essential components of atmospheric neutrinos, the result of Ref. [17] agrees with a hypothesis of zero prompt neutrino event. Therefore, in the analysis in Section 4, we do not consider the contribution of prompt neutrinos in the search for sterile neutrinos.

### 3 Some analytical treatment

In the numerical analysis in Section 4, it is useful to have analytic expressions for oscillation probabilities to understand the qualitative behavior of the energy spectrum etc. So in this section we discuss some analytic expressions for oscillation probabilities in matter with constant density. For simplicity we discuss a case without absorption, i.e.,  $B = 0$  in Eqs. (15) and (16), since the analytic expressions for oscillation probabilities with  $B \neq 0$  are complicated.

#### 3.1 Atmospheric neutrinos

In this subsection, we discuss the oscillation probabilities of atmospheric neutrinos. Upward-going atmospheric neutrinos pass through the Earth and are observed at the IceCube detector. The baseline length  $L$  is given by

$$L = -R \cos \Theta + \sqrt{(R + h)^2 - (R \sin \Theta)^2}, \quad (26)$$

where  $R$  is the Earth's radius,  $\Theta$  is the zenith angle, and  $h \sim 20$  km is the thickness of the atmosphere.

In this study, we discuss neutrinos at high energy ( $E_\nu \gtrsim 1$  TeV) with a baseline length  $L \lesssim 13000$  km. Since  $|\Delta m_{\text{atm}}^2 L/E| \ll 1$  and  $|\Delta m_{\text{sol}}^2 L/E| \ll 1$ , the condition of the one mass scale dominance is satisfied. In this case, the energy difference matrix in Eq. (18) can be approximated as

$$\mathcal{E} \simeq \text{diag}(0, 0, 0, \Delta E), \quad (27)$$

where we have defined

$$\Delta E \equiv \Delta E_{41} \quad (28)$$

for simplicity, and the matrices  $\mathcal{R}_{23}(\theta_{23}, 0)$ ,  $\mathcal{R}_{13}(\theta_{13}, \delta_1)$ ,  $\mathcal{R}_{12}(\theta_{12}, 0)$  disappear from  $U$  in Eqs. (15) and (16).

It turns out that the two cases  $\theta_{14} \neq 0$ ,  $\theta_{24} = \theta_{34} = 0$  and  $\theta_{14} = 0$ ,  $\theta_{24} \neq 0$ ,  $\theta_{34} \neq 0$  in the limit of one mass scale dominance can be reduced to a two-flavor problem. The former (latter) has a resonance in the neutrino (antineutrino) mode, so we discuss these two cases separately. In both cases, CP phases do not appear in the oscillation probability, as in the two-flavor case.

### 3.1.1 The case with $\theta_{14} \neq 0$ , and $\theta_{24} = \theta_{34} = 0$

We first consider a case where there is only one non-zero mixing angle  $\theta_{14}$ , whereas  $\theta_{24}$  and  $\theta_{34}$  vanish. In this case, there is mixing only between electron and sterile neutrinos, and Eq. (15) reduces to the one in the two-flavor case. From Eq. (76) in Appendix A, we can calculate the oscillation probability of  $\nu_e \rightarrow \nu_e$ :

$$P(\nu_e \rightarrow \nu_e) = 1 - \sin^2 2\tilde{\theta}_{14} \sin^2 \left( \frac{\Delta\tilde{E}_1 L}{2} \right), \quad (29)$$

where  $\tilde{\theta}_{14}$  and  $\Delta\tilde{E}_1$  are, respectively, defined by

$$\tan 2\tilde{\theta}_{14} = \frac{\Delta E \sin 2\theta_{14}}{\Delta E \cos 2\theta_{14} - A_e + A_s}. \quad (30)$$

$$\Delta\tilde{E}_1 = \sqrt{(\Delta E \cos 2\theta_{14} - A_e + A_s)^2 + (\Delta E \sin 2\theta_{14})^2}. \quad (31)$$

Since  $A_e - A_s \simeq A_e/2 > 0$  and  $\Delta E = \Delta m_{41}^2/(2E) > 0$ , Eq. (30) indicates that a resonance occurs only in the neutrino mode at the neutrino energy  $E = \Delta m_{41}^2/\{2(A_e - A_s)\}$ .

Moreover, it is useful to study the behavior of oscillation probabilities when considering the following:

$$\Delta m_{41}^2 \rightarrow +\infty. \quad (32)$$

If  $\Delta m_{41}^2 \rightarrow +\infty$ , then the vacuum oscillation contribution  $\Delta E$  dominates over the matter term  $A_e - A_s$  in Eq. (30), so we have  $\tilde{\theta}_{14} \rightarrow \theta_{14}$ , whereas  $\Delta\tilde{E} \rightarrow +\infty$  leads to rapid oscillation in Eq. (29). Thus we obtain

$$P(\nu_e \rightarrow \nu_e) \rightarrow 1 - \frac{1}{2} \sin^2 2\theta_{14}. \quad (33)$$

From Eq. (33), we observe that if  $\Delta m_{41}^2 \rightarrow +\infty$ , the oscillation probability  $P(\nu_e \rightarrow \nu_e)$  becomes independent of the zenith angle  $\Theta$  and neutrino energy  $E$ . The fact that  $P(\nu_e \rightarrow \nu_e)$  becomes a constant suppression as  $\Delta m_{41}^2 \rightarrow +\infty$  implies that the significance of the (3+1)-scheme with  $\theta_{14} \neq 0$  at very large  $\Delta m_{41}^2$  depends entirely on the systematic errors.

### 3.1.2 The case with $\theta_{14} = 0$ , $\theta_{24} \neq 0$ and $\theta_{34} \neq 0$

Next, we consider a case where there are two non-zero mixing angles  $\theta_{24}$  and  $\theta_{34}$ , whereas  $\theta_{14}$  vanishes. Although the (3+1)-scheme for which we perform the numerical analysis is not this case, it is instructive to see how a resonance occurs in the antineutrino mode in this case.

As explained in Appendix B, there can be a resonance in the antineutrino mode (see Eq. (96)). Therefore, we discuss the disappearance channel  $\bar{\nu}_\mu \rightarrow \bar{\nu}_\mu$ , introducing a new set of angles

$$\tan \varphi_{12} \equiv \frac{t_{34}}{s_{24}}, \quad (34)$$

$$\sin \varphi_{13} \equiv c_{24}c_{34}, \quad (35)$$

$$\tan \varphi_{23} \equiv \frac{s_{34}}{t_{24}}, \quad (36)$$

where  $c_{jk} \equiv \cos \theta_{jk}$ ,  $s_{jk} \equiv \sin \theta_{jk}$ ,  $t_{jk} \equiv \tan \theta_{jk}$ , and  $\theta_{jk}$  ( $j, k = 1, \dots, 4$ ) is the original mixing angle in the parametrization (13). The oscillation probabilities  $P(\bar{\nu}_\mu \rightarrow \bar{\nu}_\mu)$  and  $P(\bar{\nu}_\mu \rightarrow \bar{\nu}_\tau)$  can be expressed as:

$$P(\bar{\nu}_\mu \rightarrow \bar{\nu}_\mu) = 1 - C_{23}^4 \sin^2 2\tilde{\varphi}_{13} \sin^2 \left( \frac{\Delta \tilde{E}_2 L}{2} \right) - \sin^2 2\varphi_{23} \left\{ \tilde{S}_{13}^2 \sin^2 \left( \frac{\varepsilon_{2-} L}{2} \right) + \tilde{C}_{13}^2 \sin^2 \left( \frac{\varepsilon_{2+} L}{2} \right) \right\}, \quad (37)$$

$$P(\bar{\nu}_\mu \rightarrow \bar{\nu}_\tau) = \sin^2 2\varphi_{23} \left\{ \tilde{S}_{13}^2 \sin^2 \left( \frac{\varepsilon_{2-} L}{2} \right) + \tilde{C}_{13}^2 \sin^2 \left( \frac{\varepsilon_{2+} L}{2} \right) - \frac{1}{4} \sin^2 2\tilde{\varphi}_{13} \sin^2 \left( \frac{\Delta \tilde{E}_2 L}{2} \right) \right\}, \quad (38)$$

where  $\tilde{\varphi}_{13}$ ,  $\Delta \tilde{E}_2$  and  $\varepsilon_{2\mp}$  are, respectively, given by

$$\tan 2\tilde{\varphi}_{13} = \frac{\Delta E \sin 2\varphi_{13}}{\Delta E \cos 2\varphi_{13} + A_s}, \quad (39)$$

$$\Delta \tilde{E}_2 = \sqrt{(\Delta E \cos 2\varphi_{13} + A_s)^2 + (\Delta E \sin 2\varphi_{13})^2}, \quad (40)$$

$$\varepsilon_{2\mp} = \frac{\Delta E - A_s}{2} \mp \frac{1}{2} \Delta \tilde{E}_2, \quad (41)$$

and we introduced the notations  $\tilde{S}_{13} = \sin \tilde{\varphi}_{13}$ ,  $\tilde{C}_{13} = \cos \tilde{\varphi}_{13}$ ,  $S_{23} = \sin \varphi_{23}$  and  $C_{23} = \cos \varphi_{23}$ . If  $\theta_{24}$  and  $\theta_{34}$  are both small so that  $0 < s_{24} \ll 1$  and  $0 < s_{34} \ll 1$  are satisfied, from Eq. (35), we have  $0 < \pi/2 - \varphi_{13} \ll 1$ , which implies that  $2\varphi_{13} \simeq \pi$  and  $\cos 2\varphi_{13} \simeq -1$ , so that the resonance condition, in which the denominator of Eq. (39) vanishes, is possible only for antineutrinos. Notice that the denominator for neutrinos would be  $\Delta E \cos 2\varphi_{13} - A_s$ , which is negative for any value of the neutrino energy  $E > 0$ .

Now, let us consider the behavior of the oscillations probabilities  $\bar{\nu}_\mu \rightarrow \bar{\nu}_\mu$  and  $\bar{\nu}_\mu \rightarrow \bar{\nu}_\tau$  as  $\Delta m_{41}^2 \rightarrow +\infty$ , where  $\Delta E$  dominates over the matter term  $A_s$  in Eq. (39), so we have  $\tilde{\varphi}_{13} \rightarrow \varphi_{13}$ . Moreover, for the three energy differences, two of them become large whereas one remains finite:

$$\Delta \tilde{E}_2 \sim \Delta E \rightarrow +\infty. \quad (42)$$

$$\varepsilon_{2+} = \frac{\Delta E - A_s}{2} + \frac{1}{2} \Delta \tilde{E}_2 \sim \Delta E \rightarrow +\infty. \quad (43)$$

$$\begin{aligned} \varepsilon_{2-} &= \frac{\varepsilon_{2+} + \varepsilon_{2-}}{\varepsilon_{2+}} \\ &= \frac{A_s \Delta E \cos^2 \varphi_{13}}{\varepsilon_{2+}} \rightarrow A_s \cos^2 \varphi_{13}, \end{aligned} \quad (44)$$

From this,  $\sin^2(\Delta \tilde{E}_2 L/2)$  and  $\sin^2(\varepsilon_{2+} L/2)$  are averaged to yield  $1/2$ , whereas  $\sin^2(\varepsilon_{2-} L/2)$  becomes  $\sin^2(A_s \cos^2 \varphi_{13} L/2)$ , which does not depend on the neutrino energy  $E$  but



depends on the baseline length  $L$ . Thus, we obtain

$$P(\bar{\nu}_\mu \rightarrow \bar{\nu}_\mu) \rightarrow 1 - \frac{C_{23}^4}{2} \sin^2 2\varphi_{13} - \sin^2 2\varphi_{23} \left\{ S_{13}^2 \sin^2 \left( \frac{A_s \cos^2 \varphi_{13} L}{2} \right) + \frac{C_{13}^2}{2} \right\}, \quad (45)$$

$$P(\bar{\nu}_\mu \rightarrow \bar{\nu}_\tau) \rightarrow \sin^2 2\varphi_{23} \left\{ S_{13}^2 \sin^2 \left( \frac{A_s \cos^2 \varphi_{13} L}{2} \right) + \frac{C_{13}^2}{2} - \frac{1}{8} \sin^2 2\varphi_{13} \right\}, \quad (46)$$

Eq. (45) shows that, even as  $\Delta m_{41}^2 \rightarrow +\infty$ , the disappearance probability has some dependence on the zenith angle  $\Theta$  (not only  $P(\bar{\nu}_\mu \rightarrow \bar{\nu}_\mu)$  but also  $P(\nu_\mu \rightarrow \nu_\mu)$  because Eq. (45) is an even function of  $A_s$ ), which is why the IceCube has some sensitivity to  $\theta_{24}$  even at  $\Delta m_{41}^2 = 100 \text{ eV}^2$  (cf. the upper panel of FIG.19 in Ref. [14]). This phenomenon has also been known in the standard three-flavor scenario [18, 19], where the atmospheric neutrino data was accounted for to some extent, even for a low value of the mass-squared difference  $|\Delta m_{\text{atm}}^2|$ .

## 3.2 Astrophysical neutrinos

Next, we discuss neutrino oscillations of astrophysical neutrinos. We consider the following propagation process: astrophysical neutrinos start from the source and travel a long distance in outer space (in vacuum), then reach and pass through the Earth (in matter), and are finally observed at IceCube. In the following, we develop formulae for calculating the oscillation probabilities in this process.

Calculating these oscillation probabilities is similar to that of the day-night effect of solar neutrinos. We denote  $L_0$  as the astronomical travel distance of astrophysical neutrinos in outer space, and  $L$  as the propagation distance of astrophysical neutrinos inside the Earth. Because  $|\Delta m_{ij}^2 L_0 / E| \gg 1$  ( $i, j = 1, \dots, 4$ ), to a good approximation, we can assume  $L_0 \rightarrow +\infty$ . Further, we denote  $T$  as the transition matrix of the neutrino flavor state inside the Earth. Then we have the formulae of oscillation probabilities in the entire propagation process:

$$\begin{aligned} P(\nu_\alpha \rightarrow \nu_\beta) &= \lim_{L_0 \rightarrow +\infty} \sum_{\rho j} T_{\beta\rho} U_{\rho j} \exp(-iL_0 E_j) U_{j\alpha}^{-1} \\ &\quad \times \left( \sum_{\sigma n} T_{\beta\sigma} U_{\sigma n} \exp(-iL_0 E_n) U_{n\alpha}^{-1} \right)^* \\ &= \lim_{L_0 \rightarrow +\infty} \sum_{\rho \sigma j n} T_{\beta\rho} T_{\beta\sigma}^* U_{\rho j} U_{\sigma n}^* \exp(iL_0 \Delta E_{nj}) U_{\alpha j}^* U_{\alpha n} \\ &= \sum_{\rho \sigma n} T_{\beta\rho} T_{\beta\sigma}^* U_{\rho n} U_{\sigma n}^* |U_{\alpha n}|^2 \quad (\alpha, \beta = e, \mu, \tau, s), \end{aligned} \quad (47)$$

where we have used the unitary condition of the PMNS matrix  $U$ .

### 3.2.1 The case with $\theta_{14} \neq 0$ , and $\theta_{24} = \theta_{34} = 0$

The flavor ratio of neutrinos in the case of  $\theta_{14} \neq 0$ ,  $\theta_{24} = \theta_{34} = 0$  is given by the following (for a detailed description, see Appendix C):

$$F(\nu_e) : F(\nu_\mu) : F(\nu_\tau) : F(\nu_s) \simeq 1 - |T_{14}|^2 : 1 : 1 : |T_{14}|^2, \quad (48)$$

where  $|T_{14}|^2$  is defined as

$$|T_{14}|^2 = \sin^2 2\tilde{\theta}_{14} \sin^2 \left( \frac{\Delta\tilde{E}_1 L}{2} \right), \quad (49)$$

$\tilde{\theta}_{14}$  and  $\Delta\tilde{E}_1$  are defined by Eqs. (30) and (31), respectively, and  $L$  is the path length of astrophysical neutrinos inside the Earth. Note that the factor  $|T_{14}|^2$  and hence the flavor ratio (48) have a nontrivial dependence on the neutrino energy  $E$  especially near the resonance region  $E \sim \Delta m_{41}^2 / \{2(A_e - A_s)\}$ .

### 3.2.2 The case with $\theta_{14} = 0$ , $\theta_{24} \neq 0$ and $\theta_{34} \neq 0$

In the case with  $\theta_{14} = 0$ ,  $\theta_{24} \neq 0$ , and  $\theta_{34} \neq 0$ , as described in detail in Appendix D, the flavor ratio of *antineutrinos* is expressed as follows:

$$F(\bar{\nu}_e) : F(\bar{\nu}_\mu) : F(\bar{\nu}_\tau) : F(\bar{\nu}_s) \simeq 1 : 1 - C_{23}^2 |T_{44}|^2 : 1 - S_{23}^2 |T_{44}|^2 : 1 - |T_{44}|^2, \quad (50)$$

where  $|T_{44}|^2$  is defined as

$$|T_{44}|^2 = 1 - \sin^2 2\tilde{\varphi}_{13} \sin^2 \left( \frac{\Delta\tilde{E}_2 L}{2} \right), \quad (51)$$

$C_{23} \equiv \cos \varphi_{23}$ ,  $S_{23} \equiv \sin \varphi_{23}$ , the new mixing angles  $\varphi_{ij}$  ( $i, j = 1, 2, 3$ ) are defined in Eqs. (34), (35), (36),  $\tilde{\varphi}_{13}$  and  $\Delta\tilde{E}_2$  are defined by Eqs. (39) and (40), respectively, and  $L$  is the path length of astrophysical neutrinos inside the Earth. Notice that the factor  $|T_{44}|^2$  and therefore the flavor ratio (50) also have a nontrivial dependence on the neutrino energy  $E$  especially near the resonance region  $E \sim \Delta m_{41}^2 / (2A_s)$ .

## 4 Numerical analysis of shower events

In this section, for simplicity, we perform numerical analysis to obtain the sensitivity to  $\theta_{14}$  as a function of  $\Delta m_{41}^2$  in the (3+1)-scheme, assuming  $\theta_{24} = \theta_{34} = 0$ . As shown in Section 3, the case with  $\theta_{14} \neq 0, \theta_{24} = \theta_{34} = 0$  has a resonance in the neutrino mode, whereas the case with  $\theta_{14} = 0, \theta_{24} \neq 0, \theta_{34} \neq 0$  has one in the antineutrino mode. If we turn on small  $\theta_{24}$  and  $\theta_{34}$ , the resonance in the neutrino mode has small perturbation with respect to  $\theta_{24}$  and  $\theta_{34}$ , and we expect that our conclusion does not change significantly.

We assume that the numbers of events at an IceCube-like neutrino telescope are given by extrapolating those in FIG.6 in Ref. [17], i.e., they are given by a factor (volume of the IceCube-like detector)  $\times$  (number of days of measurement) / [(volume of the IceCube)  $\times$  (332 days)]. The figure shows the energy spectrum of various numbers of shower events for 332 days at IceCube. They comprise conventional atmospheric  $\nu_e + \bar{\nu}_e$ , conventional atmospheric  $\nu_\mu + \bar{\nu}_\mu$ , (which look like shower events even after the experimental cuts), astrophysical  $\nu_\beta + \bar{\nu}_\beta$  ( $\beta = e, \mu, \tau$ ), and cosmic ray muons. Note that the IceCube collaboration concluded that zero prompt neutrino event is consistent with their data, so we also assume that there is no prompt neutrino event in our analysis.

## 4.1 Numbers of events

The neutrinos observed at an IceCube-like detector are either atmospheric or astrophysical, and are expected to be produced mainly from pion and kaon decays. So, it is expected that there are only  $\nu_e + \bar{\nu}_e$  and  $\nu_\mu + \bar{\nu}_\mu$  at the production point. However, during neutrino propagation, the processes  $\nu_\alpha \rightarrow \nu_\tau$  ( $\alpha = e, \mu$ ) and  $\bar{\nu}_\alpha \rightarrow \bar{\nu}_\tau$  ( $\alpha = e, \mu$ ) exist in general neutrino mixing. For atmospheric neutrinos, in the standard three-flavor mixing scenario or (3+1)-scheme where the only non-zero sterile neutrino mixing angle is  $\theta_{14}$ , there are very few  $\nu_\tau + \bar{\nu}_\tau$  from the conventional atmospheric neutrinos through the oscillations  $\nu_\mu \rightarrow \nu_\tau$  and  $\bar{\nu}_\mu \rightarrow \bar{\nu}_\tau$  because the oscillation probability is very small:  $P(\nu_\mu \rightarrow \nu_\tau) \simeq P(\bar{\nu}_\mu \rightarrow \bar{\nu}_\tau) \simeq \sin^2 2\theta_{23} \sin^2(\Delta m_{31}^2 L/4E) \ll 1$  for  $E > 1$  TeV,  $L \lesssim 2R$ , where  $R$  is the Earth's radius. Meanwhile, for astrophysical neutrinos, we have  $\nu_\tau + \bar{\nu}_\tau$  because of oscillations with an astronomical baseline length [20].

Thus, the number of events ( $N_{jk}(\nu_\beta)$  for  $\nu_\beta$  and  $N_{jk}(\bar{\nu}_\beta)$  for  $\bar{\nu}_\beta$ ) for the energy bin ( $E_j < E < E_{j+1}$ ) and zenith angle bin ( $\cos \Theta_k < \cos \Theta < \cos \Theta_{k+1}$ ) can be expressed in terms of the flux  $\Phi(\nu_\alpha, E', \Theta')$ , the cross section [21] ( $\sigma_X(E')$  for neutrinos and  $\bar{\sigma}_X(E')$  for antineutrinos, for CC ( $X = CC$ ) and NC ( $X = NC$ ) interactions, respectively) and the detection efficiency  $\epsilon_X(E, \nu_\beta)$  ( $X = CC, NC$ ) as follows:

$$\begin{aligned}
& \left\{ \begin{array}{l} N_{jk}(\nu_\beta) \\ N_{jk}(\bar{\nu}_\beta) \end{array} \right\} \\
&= \int_{\log_{10} E_j}^{\log_{10} E_{j+1}} d \log_{10} E \int_{\cos \Theta_j}^{\cos \Theta_{j+1}} d \cos \Theta \int_{-\infty}^{\infty} d \log_{10} E' \int_{-1}^1 d \cos \Theta' \\
&\quad \times R_e(E, E', \Delta_e(E)) R_z(\Theta, \Theta', \Delta_z(E)) \\
&\quad \times \sum_{\alpha} \sum_{X=CC, NC} \left\{ \begin{array}{l} \Phi(\nu_\alpha, E', \Theta') P(\nu_\alpha \rightarrow \nu_\beta) \sigma_X(E') \epsilon_X(E', \nu_\beta) \\ \Phi(\bar{\nu}_\alpha, E', \Theta') P(\bar{\nu}_\alpha \rightarrow \bar{\nu}_\beta) \bar{\sigma}_X(E') \epsilon_X(E', \bar{\nu}_\beta) \end{array} \right\} \quad (52)
\end{aligned}$$

$R_e$  and  $R_z$  represent the resolution functions in the neutrino energy and zenith angle, respectively:

$$\begin{aligned}
R_e(E, E', \Delta_e(E)) &\equiv \frac{1}{\sqrt{\pi} \Delta_e(E)} \exp \left\{ -\frac{(\log_{10} E - \log_{10} E')^2}{\Delta_e(E)^2} \right\} \\
R_z(\Theta, \Theta', \Delta_z(E)) &\equiv N(\Theta) \exp \left\{ -\frac{(\cos \Theta - \cos \Theta')^2}{\Delta_z(E)^2} \right\} \\
N(\Theta) &\equiv \left[ \int_{-1}^1 d \cos \Theta' \exp \left\{ -\frac{(\cos \Theta - \cos \Theta')^2}{\Delta_z(E)^2} \right\} \right]^{-1} \quad (53)
\end{aligned}$$

where  $E'$  and  $\Theta'$  are the true neutrino energy and zenith angle, respectively, whereas  $E$  and  $\Theta$  are the reconstructed ones, respectively. We use the energy resolution  $\Delta_e(E)$  and the zenith angle resolution  $\Delta_z(E)$  which are given by the blue curve “iterative CREDO” in FIG.5 in Ref. [17].

### 4.1.1 Atmospheric neutrinos

We use the atmospheric neutrino flux in Ref. [22] in our analysis. However, the flux in Ref. [22] is given only up to 10 TeV, and we need the flux up to  $\mathcal{O}(100 \text{ TeV})$  for

our analysis. Therefore, we adopt the following empirical formula in Ref. [23] for the atmospheric neutrino flux, and extrapolate it up to  $\mathcal{O}(100 \text{ TeV})$ :

$$\left\{ \begin{array}{l} \Phi^{\text{atm}}(\nu_\mu, E, \Theta) \\ \Phi^{\text{atm}}(\bar{\nu}_\mu, E, \Theta) \end{array} \right\} = \frac{2.85 \cdot 10^{-2}}{\text{cm}^2 \text{ sr s GeV}} \cdot A \cdot \left( \frac{E}{\text{GeV}} \right)^{-\gamma} \times \left( \frac{1}{1 + 6 E \cos \Theta^*/121 \text{ GeV}} + \frac{0.213}{1 + 1.44 E \cos \Theta^*/897 \text{ GeV}} \right) \quad (54)$$

$$\left\{ \begin{array}{l} \Phi^{\text{atm}}(\nu_e, E, \Theta) \\ \Phi^{\text{atm}}(\bar{\nu}_e, E, \Theta) \end{array} \right\} = \frac{2.4 \cdot 10^{-3}}{\text{cm}^2 \text{ sr s GeV}} \cdot A \cdot \left( \frac{E}{\text{GeV}} \right)^{-\gamma} \times \left( \frac{0.05}{1 + 1.5 E \cos \Theta^*/897 \text{ GeV}} + \frac{0.185}{1 + 1.5 E \cos \Theta^*/194 \text{ GeV}} + \frac{11.4 E^{\zeta(\Theta)}}{1 + 1.21 E \cos \Theta^*/121 \text{ GeV}} \right) \quad (55)$$

where the cosine of the zenith angle  $\Theta$  is modified as that of the effective one  $\Theta^*$  by considering the curvature of the atmosphere:

$$\cos \Theta^* = \sqrt{\frac{\cos^2 \Theta + p_1^2 + p_2 \cos^3 \Theta + p_4 \cos^5 \Theta}{1 + p_1^2 + p_2 + p_4}} \\ (p_1, p_2, p_3, p_4, p_5) = (0.102573, -0.068287, 0.958633, 0.0407253, 0.817285).$$

$A$  is the normalization, given by  $A = 0.646$  for  $\nu_\mu, \bar{\nu}_\mu$  and  $A = 0.828$  for  $\nu_e, \bar{\nu}_e$ .  $\gamma$  is the spectral index for atmospheric neutrinos, and the flux for each flavor ( $\nu_\mu, \bar{\nu}_\mu, \nu_e$  and  $\bar{\nu}_e$ ) in Ref. [22] is best reproduced by  $\gamma = 2.680$  (for  $\nu_\mu$ ),  $2.696$  (for  $\bar{\nu}_\mu$ ),  $2.719$  (for  $\nu_e$ ), and  $2.741$  (for  $\bar{\nu}_e$ ). Hence, we use Eqs. (54) and (55) with these values for  $\gamma$  up to the neutrino energy  $E \lesssim 1 \text{ PeV}$ .  $\zeta$  in Eq. (55) is given by

$$\zeta = a + b \log_{10}(E/\text{GeV}) \\ a = \max(0.11 - 2.4 \cos \Theta, -0.46 - 0.54 \cos \Theta) \\ b = \min(-0.22 + 0.69 \cos \Theta, -0.01 + 0.01 \cos \Theta)$$

#### 4.1.2 Detection efficiency for shower events

The detection efficiency  $\epsilon_X(E, \nu_\beta)$  ( $\beta = e, \mu; X = CC, NC$ ) in Eq. (52) for shower events can be deduced from the number of shower events of atmospheric neutrinos given in Ref. [17], if we make the following assumptions:

- (i) The detection efficiencies for neutrinos and antineutrinos are the same.

$$\epsilon_X(E, \nu_\beta) = \epsilon_X(E, \bar{\nu}_\beta) \quad (\beta = e, \mu, \tau; X = CC, NC) \quad (56)$$

- (ii) The energy dependencies of  $\epsilon_{NC}(E, \nu_e)$  and  $\epsilon_{CC}(E, \nu_e)$  are the same, i.e.,

$$\epsilon_{NC}(E, \nu_e) = \text{const.} \epsilon_{CC}(E, \nu_e) \quad (57)$$

- (iii) The detection efficiencies  $\epsilon_{NC}(E, \nu_\beta)$  for all flavors  $\beta = e, \mu$ , and  $\tau$  are the same.

$$\epsilon_{NC}(E, \nu_e) = \epsilon_{NC}(E, \nu_\mu) = \epsilon_{NC}(E, \nu_\tau) \quad (58)$$

- (iv) The detection efficiency for hadronic shower events from  $\nu_\tau$  and  $\bar{\nu}_\tau$  is the same as that for electromagnetic shower events from  $\nu_e$  and  $\bar{\nu}_e$ . Since 65% (18%) of tau decay is hadronic (electromagnetic) [1], this assumption implies

$$\epsilon_{CC}(E, \nu_\tau) = 0.83 \epsilon_{CC}(E, \nu_e). \quad (59)$$

From TABLE I in Ref. [17], the numbers of events for 332 days at IceCube are 198 (CC) + 17 (NC) for  $\nu_e + \bar{\nu}_e$ , 387 (CC) + 258 (NC) for  $\nu_\mu + \bar{\nu}_\mu$ , 115 for cosmic ray muons, and 103 for astrophysical  $\nu_\beta + \bar{\nu}_\beta$  ( $\beta = e + \mu + \tau$ ). Since we know the flux of conventional atmospheric neutrinos and the cross section at each energy, the CC and NC numbers of events for  $\nu_e + \bar{\nu}_e$  along with assumptions (i) and (ii) allow us to deduce the detection efficiency for  $\epsilon_{CC}(E, \nu_e)$  and  $\epsilon_{NC}(E, \nu_e)$ , where they are extrapolated up to the neutrino energy  $E \lesssim 10$  PeV. Then, from the CC and NC numbers of events for  $\nu_\mu + \bar{\nu}_\mu$  with assumptions (iii), we can deduce  $\epsilon_{CC}(E, \nu_\mu)$ . Thus, we obtain  $\epsilon_{CC}(E, \nu_e)$ ,  $\epsilon_{NC}(E, \nu_e)$  and  $\epsilon_{CC}(E, \nu_\mu)$ , and they are depicted in an arbitrary unit in Figure 1. Assumption (iv) can be used to deduce  $\epsilon_{CC}(E, \nu_\tau)$  if there are  $\nu_\tau + \bar{\nu}_\tau$ .

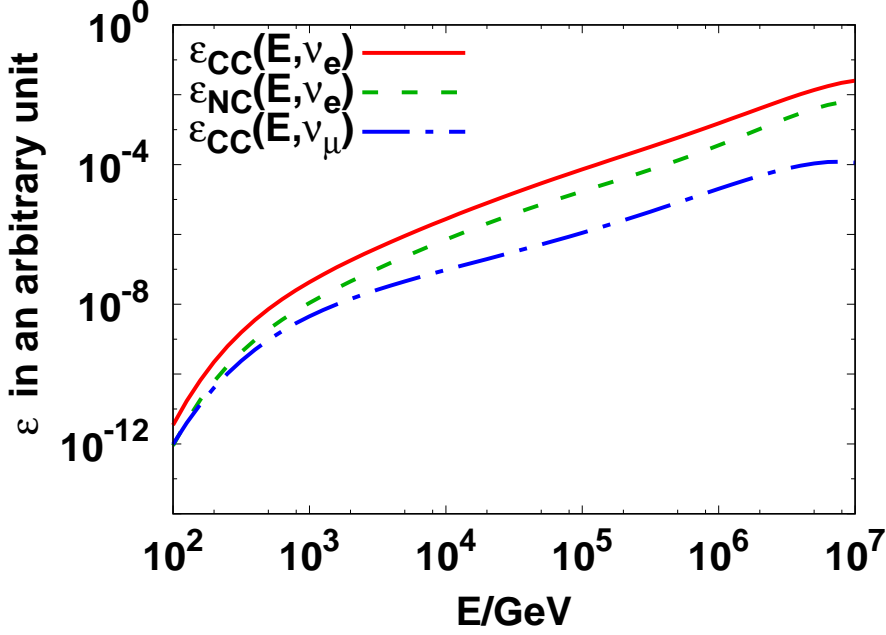


Figure 1: Detection efficiency  $\epsilon_{CC}(E, \nu_e)$ ,  $\epsilon_{NC}(E, \nu_e)$  and  $\epsilon_{CC}(E, \nu_\mu)$ , deduced from FIG.6 in Ref. [17], the flux in Refs. [22] and [23], the cross section in Ref. [21], and assumptions (i) - (iii) in this article. The absolute magnitude is arbitrary, and we fix the normalization so that the total numbers of events coincide with those in Ref. [17].

### 4.1.3 Astrophysical neutrinos

The flux of astrophysical neutrinos is assumed to be isotropical, and the ratios  $\Phi^{\text{ast}}(\nu_\mu)/\Phi^{\text{ast}}(\nu_e)$  and  $\Phi^{\text{ast}}(\bar{\nu}_\mu)/\Phi^{\text{ast}}(\bar{\nu}_e)$  at the production point are assumed to be 2:

$$\begin{aligned}\Phi^{\text{ast}}(\nu_\mu, E, \Theta) &= \Phi^{\text{ast}}(\bar{\nu}_\mu, E, \Theta) = 2\Phi^{\text{ast}}(\nu_e, E, \Theta) = 2\Phi^{\text{ast}}(\bar{\nu}_e, E, \Theta) \\ &= \frac{1}{3}\Phi_0^{\text{ast}}\left(\frac{E}{100\text{TeV}}\right)^{-\gamma}\end{aligned}\quad (60)$$

where  $\gamma$  is the astrophysical spectral index, and  $\Phi_0^{\text{ast}}$  is the total flux of astrophysical neutrinos at  $E=100$  TeV.<sup>3</sup> We adopt the reference value  $\gamma=2.4$  used in Ref. [17].

If there is no enhancement of the sterile mixing angle  $\theta_{14}$  due to the matter effect in the Earth, the oscillation probabilities are approximately given by those in vacuum in the limit of an infinite baseline length, and

$$\begin{aligned}&\sum_{\alpha=e,\mu}\Phi^{\text{ast}}(\nu_\alpha, E', \Theta')P(\nu_\alpha \rightarrow \nu_e) \\ &\simeq \sum_{\alpha=e,\mu}\Phi^{\text{ast}}(\nu_\alpha, E', \Theta')P(\nu_\alpha \rightarrow \nu_\mu) \\ &\simeq \sum_{\alpha=e,\mu}\Phi^{\text{ast}}(\nu_\alpha, E', \Theta')P(\nu_\alpha \rightarrow \nu_\tau),\end{aligned}\quad (61)$$

as was pointed out in Ref. [20]. Meanwhile, if there is an enhancement of the sterile mixing angle  $\theta_{14}$ , Eq. (61) is modified for the energy range in which the enhancement of the effective mixing angle  $\theta_{14}$  occurs. Particularly, if the sterile mixing angle  $\theta_{14}$  and mass-squared difference lie in a suitable range, then the flavor ratio  $(\nu_e + \bar{\nu}_e) : (\nu_\mu + \bar{\nu}_\mu) : (\nu_\tau + \bar{\nu}_\tau) = 1 - |T_{14}|^2/2 : 1 : 1$ , (where the flavor ratio of neutrinos is given by Eq. (48), and the flavor ratio of antineutrinos is 1:1:1 in the absence of resonance), may be observed, instead of the standard flavor ratio [20]  $(\nu_e + \bar{\nu}_e) : (\nu_\mu + \bar{\nu}_\mu) : (\nu_\tau + \bar{\nu}_\tau) = 1:1:1$ . This deviation depends on the neutrino energy, and it can be a signal to search for sterile neutrino oscillations. Although we discuss only the case with  $\theta_{14} \neq 0$ ,  $\theta_{24} = \theta_{34} = 0$  in this study, if the astrophysical neutrino events can be separated from those of atmospheric neutrinos, the energy dependence of the flavor ratio is in general one of the signatures of sterile neutrino oscillations for the range  $1 \text{ eV}^2 \lesssim \Delta m_{41}^2 \lesssim 100 \text{ eV}^2$ .

## 4.2 $\chi^2$

In this study, we examine whether the numbers of shower events predicted by the (3+1)-scheme with  $\theta_{14} \neq 0$  can be distinguished from those without sterile neutrino oscillation, i.e., those with the standard three-flavor framework with the central value of the oscillation parameters given in Eqs. (2)-(8) with NO. To evaluate the significance between the number of events with  $\theta_{14} \neq 0$  and the one without non-zero

---

<sup>3</sup>If there is no enhancement of the sterile mixing angle  $\theta_{14}$  due to the matter effect in the Earth, then each flux at  $E=100$  TeV is  $\Phi^{\text{ast}}(\nu_e) \simeq \Phi^{\text{ast}}(\bar{\nu}_e) \simeq \Phi^{\text{ast}}(\nu_\mu) \simeq \Phi^{\text{ast}}(\bar{\nu}_\mu) \simeq \Phi^{\text{ast}}(\nu_\tau) \simeq \Phi^{\text{ast}}(\bar{\nu}_\tau) \simeq \Phi_0^{\text{ast}}/6$ , so that the total flux is approximately  $\Phi_0^{\text{ast}}$ .

$\theta_{14}$ , we use the following Poisson likelihood chi-square:

$$\chi_0^2 = 2 \sum_{j,k} \left[ Y_{jk} - N_{jk} - N_{jk} \log \left( \frac{Y_{jk}}{N_{jk}} \right) \right], \quad (62)$$

where  $j$  represents the  $j$ -th zenith angle bin  $((j-11)/10 \leq \cos \Theta \leq (j-10)/10, 1 \leq j \leq 20)$ , and  $k$  represents the  $k$ -th energy bin  $((j+7)/4 \leq \log_{10}(E/\text{GeV}) \leq (j+8)/4, 1 \leq k \leq 16)$ . Moreover,

$$Y_{jk} = (1 + \alpha_1) [N_{jk}^{\text{atm}}(\nu_e + \bar{\nu}_e; \theta_{14}) + N_{jk}^{\text{atm}}(\nu_\mu + \bar{\nu}_\mu; 0)] \\ + (1 + \alpha_2) N_{jk}^{\text{cr}-\mu} + (1 + \alpha_3) N_{jk}^{\text{ast}}(\theta_{14}) \quad (63)$$

and

$$N_{jk} = N_{jk}^{\text{atm}}(\nu_e + \bar{\nu}_e; 0) + N_{jk}^{\text{atm}}(\nu_\mu + \bar{\nu}_\mu; 0) \\ + N_{jk}^{\text{cr}-\mu} + N_{jk}^{\text{ast}}(0), \quad (64)$$

where  $\alpha_1, \alpha_2$  and  $\alpha_3$  are three pull parameters;  $N_{jk}^{\text{atm}}(\nu_e + \bar{\nu}_e; \theta_{14})$  and  $N_{jk}^{\text{atm}}(\nu_e + \bar{\nu}_e; 0)$  represent the number of events of atmospheric electron neutrinos with and without *sterile* neutrino oscillation (i.e.,  $\theta_{14} \neq 0$  or  $\theta_{14} = 0$ ), respectively, while assuming all three-flavor oscillation parameters as the central value given in Eqs. (2)-(8) with NO in both cases;  $N_{jk}^{\text{atm}}(\nu_\mu + \bar{\nu}_\mu; 0)$  represents the number of events of atmospheric muon neutrinos without *sterile* neutrino oscillation,  $N_{jk}^{\text{ast}}(\theta_{14})$  and  $N_{jk}^{\text{ast}}(0)$  represent the number of events of astrophysical neutrinos with and without *sterile* neutrino oscillation, respectively,  $N_{jk}^{\text{cr}-\mu}$  stands for the number of events of cosmic ray muons. Notice that in all numbers of events  $N_{jk}^*(\theta_{14})$  and  $N_{jk}^*(0)$ , the effects of the standard three-flavor oscillation are considered, since we are interested in the difference between the numbers of shower events with the standard three-flavor oscillation scenario and those with the (3+1)-scheme.

The total  $\chi^2$  is defined as follows:

$$\chi^2 = \min_{\alpha_1, \alpha_2, \alpha_3} \left[ \chi_0^2 + \left( \frac{\alpha_1}{\sigma_1} \right)^2 + \left( \frac{\alpha_2}{\sigma_2} \right)^2 + \left( \frac{\alpha_3}{\sigma_3} \right)^2 \right], \quad (65)$$

where  $\sigma_1, \sigma_2$  and  $\sigma_3$  are the three systematic errors for atmospheric neutrinos, cosmic ray muons, and astrophysical neutrinos, respectively. In this study, we set  $\sigma_1 = \sigma_2 = \sigma_3 = 0.4$  for simplicity.<sup>4</sup> In (65) we fix the three-flavor oscillation parameters and assume the central value given in Eqs. (2)-(8) with Normal Ordering. The reason that we do not marginalize  $\chi^2$  with respect to the three-flavor oscillation parameters is that we are interested in fitting the energy spectrum with a dip (i.e., the one with non-zero  $\theta_{14}$ ) to that without a dip, and variations with respect to the three-flavor oscillation parameters are not expected to affect this fitting. Thus,  $\chi^2$  becomes a function of  $\theta_{14}$  and  $\Delta m_{41}^2$ .

---

<sup>4</sup>Although various systematic errors are given in Ref. [14], in our analysis, for simplicity, we consider only the overall normalization for the atmospheric neutrinos ( $\sigma_1$ ), astrophysical neutrinos ( $\sigma_3$ ), and cosmic ray muons ( $\sigma_2$ ). The reference values quoted in Ref. [14] are  $\sigma_1 = 0.4$  and  $\sigma_3 = 0.36$ , but we could not find the one for  $\sigma_2$ . For simplicity, we assumed that all of them are 0.4. Implications of this choice will be discussed in Section 5.

### 4.3 Sensitivity

We use the number of events mentioned in (4.1) and evaluate  $\chi^2$  in Eq. (65). The region with  $\chi^2 > 4.61$  represents the region in which the hypothesis with  $\theta_{14} \neq 0$  can be excluded at 90%CL, and it is depicted in the  $(\theta_{14}, \Delta m_{41}^2)$ -plane in Figure 2. From Figure 2, if we use the number of events observed for more than 100 years with the present IceCube detector, the sensitivity can be better than the one given by DayaBay+Bugey at 90% CL [10] for  $1 \text{ eV}^2 \lesssim \Delta m_{41}^2 \lesssim 100 \text{ eV}^2$ . To achieve this sensitivity in the near future, we must increase the volume of the detector to get more numbers of events. We also observe from Figure 2 that the sensitivity to  $\Delta m_{41}^2$  is saturated for  $\Delta m_{41}^2 \gtrsim 100 \text{ eV}^2$ . Figure 3 shows the dependence of the oscillation probability  $P(\nu_e \rightarrow \nu_e)$ , which is calculated numerically by considering the absorption effect  $B$  in Eq. (15), as a function of the neutrino energy  $E$ . To see the dip, realized by the neutrino energy  $E_{\text{dip}} = \Delta m_{41}^2 / \{2(A_e - A_s)\}$ ,  $E_{\text{dip}} \lesssim 500 \text{ TeV}$  must be satisfied, and this condition yields  $\Delta m_{41}^2 \lesssim 100 \text{ eV}^2$ .

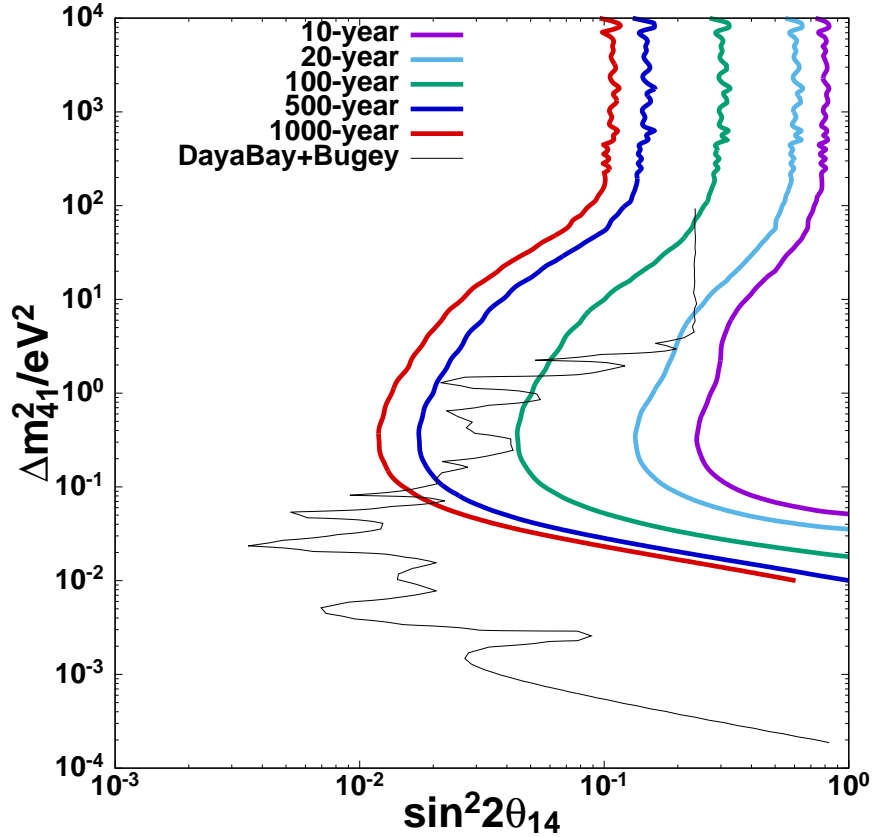


Figure 2: The expected excluded region from the shower events of the IceCube experiment for data size 10, 20, 100, 500, and 1000 years. The bound at 90% CL from the combined analysis of the Bugey3 and Daya Bay experiments [10] is also shown.



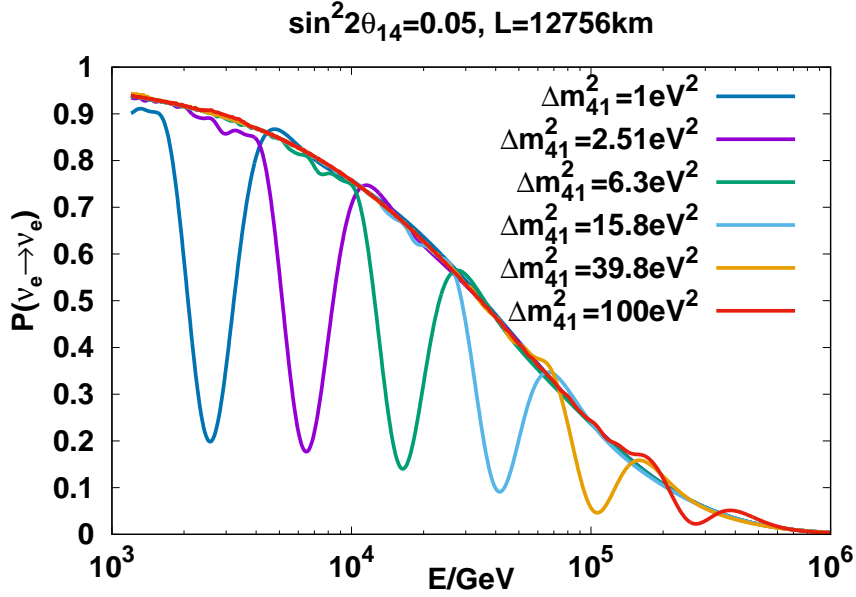


Figure 3: Oscillation probability  $P(\nu_e \rightarrow \nu_e)$  as a function of the neutrino energy  $E$  for various values of  $\Delta m_{41}^2$  in the case of  $\sin^2 2\theta_{14} = 0.05$  and the baseline length  $L = 12756$  km (= the diameter of the Earth). For  $E \gtrsim 100$  TeV, the probability decreases because of the absorption effect of neutrino.

Figure 4 shows the contribution of atmospheric and astrophysical neutrinos to the sensitivity expected by observation for 500 years at the present IceCube. We observe that atmospheric neutrinos contribute more to the sensitivity than astrophysical neutrinos because the number of events of the former is larger. Moreover, the peak of the sensitivity is obtained at  $\Delta m_{41}^2 \sim 0.1$  eV<sup>2</sup> ( $\Delta m_{41}^2 \sim 1$  eV<sup>2</sup>) for atmospheric (astrophysical) neutrinos, which is because the number of events of atmospheric neutrinos (astrophysical neutrinos) has a peak at  $E \sim 1$  TeV ( $E \sim 10$  TeV) in the energy spectrum (cf. FIG.6 in Ref. [17]), and the condition for  $\Delta m_{41}^2$  to have the dip (the denominator of Eq. (72) vanishes) leads to  $\Delta m_{41}^2 \sim 0.1$  eV<sup>2</sup> ( $\Delta m_{41}^2 \sim 1$  eV<sup>2</sup>).

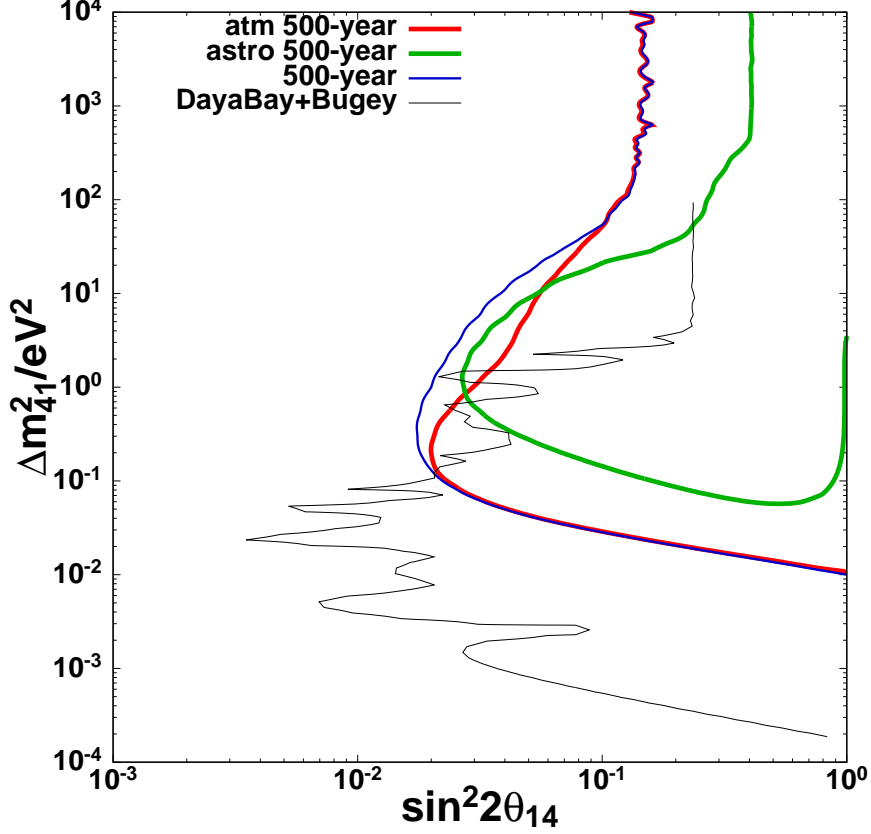


Figure 4: Hypothetical excluded region from the shower events of the IceCube experiment for 500 years, assuming only atmospheric neutrinos (red curve) or only astrophysical neutrinos (green curve), where the thin blue curve stands for the region with both atmospheric and astrophysical neutrinos for 500 years. The bound from the combined analysis of the Bugey3 and the Daya Bay experiments [10] is also shown (the thin black curve).

We note in passing that the curve from astrophysical neutrinos in Figure 4 has two intersections with a straight line  $\Delta m_{41}^2 = \text{constant}$  for  $0.06 \text{ eV}^2 \lesssim \Delta m_{41}^2 \lesssim O(1) \text{ eV}^2$ , i.e., there are two solutions of  $\chi^2 = 4.61$  for a fixed value of  $\Delta m_{41}^2$  in this region of  $\Delta m_{41}^2$ , which can be qualitatively understood as follows. As described in Appendix E, as  $\theta_{14} \rightarrow \pi/4$ , if  $\Delta E \equiv \Delta m_{41}^2/(2E) \ll |A_e - A_s|$ , the  $\nu_e$  flux becomes approximately independent of the neutrino energy  $E$  and baseline length  $L$  in the Earth. In this case, if the systematic error is not very small, the suppression due to neutrino oscillation is constant and the data may be fit by considering the overall normalization uncertainty. Meanwhile, if  $\Delta m_{41}^2$  becomes large, the condition  $\Delta m_{41}^2/(2E) \ll |A_e - A_s|$  is no longer satisfied, and the above argument does not hold. This argument qualitatively explains the behavior of the curve from astrophysical neutrinos in Figure 4.

## 5 Conclusions

In this study we showed that a future neutrino telescope facility, whose volume is at least 10 times as large as that of IceCube, can improve sensitivity to  $\theta_{14}$  by running for 10 years for  $1 \text{ eV}^2 \lesssim \Delta m_{41}^2 \lesssim 100 \text{ eV}^2$  in the (3+1)-scheme.

We have assumed that  $\theta_{24} = \theta_{34} = 0$  in our numerical analysis. If we turn on small  $\theta_{24}$  and  $\theta_{34}$ , the resonance in the neutrino mode has small perturbation with respect to  $\theta_{24}$  and  $\theta_{34}$ , and we expect that our conclusion do not change very much.

Although the variety of systematic errors in this study is smaller than that in Ref. [14], it is not expected to significantly affect the sensitivity to  $\sin^2 2\theta_{14}$  at the peak, since the sensitivity is mainly given by the energy spectrum's shape. What is significantly affected by the details of the systematic errors is the behavior for  $\Delta m_{41}^2 \gtrsim 100 \text{ eV}^2$ , because the oscillation probability in the region is expected to be averaged out to constant, and the details of the overall normalization significantly differ. So, the sensitivity to  $\sin^2 2\theta_{14}$  for  $\Delta m_{41}^2 \gtrsim 100 \text{ eV}^2$  is expected to depend on the details of the systematic errors, and more careful analysis would be required.

In our analysis, we assumed that there is no prompt neutrino event. If the volume of the future detector is increased, there can be a small contribution of prompt neutrino events for the neutrino energy  $E \gtrsim 10^{4.5} \text{ GeV}$ . However, from the result of Ref. [17] in which the data agree with a hypothesis of zero prompt neutrino event, the contribution from prompt neutrinos is expected to be much smaller than that of astrophysical neutrinos. Therefore, we expect that our results are not significantly altered even if the contribution from prompt neutrinos is considered.

We studied only the shower events for simplicity. If we combine the track and shower events, we can even give stronger constraints on the sterile mixing angles. In the presence of all non-zero sterile mixing angles, it is expected that we can also see a dip in the antineutrino disappearance channel  $\bar{\nu}_\mu \rightarrow \bar{\nu}_\mu$  at the same energy region as that in neutrino disappearance channel  $\nu_e \rightarrow \nu_e$ . This dip can be observed in the track events, and it gives us a constraint on  $\varphi_{13} = \sin^{-1}(c_{24}c_{34})$ , so we could obtain more information on the sterile mixing angles than in this study.

In summary, we emphasize that measurements of high energy neutrinos at a neutrino telescope have a potential advantage over low energy short baseline experiments in investigating sterile neutrino oscillations for  $1 \text{ eV}^2 \lesssim \Delta m_{41}^2 \lesssim 100 \text{ eV}^2$ , if the volume of the detector is at least 10 times as large as that of IceCube.

## Acknowledgements

This research was partly supported by a Grant-in-Aid for Scientific Research of the Ministry of Education, Science and Culture, under Grants No. 18K03653, No. 18H05543 and No. 21K03578.

## Appendix

### A Derivation of Eq. (29) in the case of $\theta_{14} \neq 0$ , and $\theta_{24} = \theta_{34} = 0$

In this Appendix, we discuss oscillations of atmospheric neutrinos for  $\theta_{14} \neq 0$ , and  $\theta_{24} = \theta_{34} = 0$ . Since  $\nu_\mu$  and  $\nu_\tau$  are decoupled from  $\nu_e$  and  $\nu_s$ , the system can be effectively described by the two-flavor framework. The only remaining CP phase  $\delta_2$  in Eq. (13) disappears by absorbing in the flavor eigenstate  $\nu_\alpha$  ( $\alpha = e, s$ ). Thus, we express the evolution equation as follows:

$$i \frac{d}{dt} \begin{pmatrix} \nu_e \\ \nu_s \end{pmatrix} = \left[ U_1 \begin{pmatrix} 0 & 0 \\ 0 & \Delta E \end{pmatrix} U_1^{-1} + \begin{pmatrix} A_e & 0 \\ 0 & A_s \end{pmatrix} \right] \begin{pmatrix} \nu_e \\ \nu_s \end{pmatrix}, \quad (66)$$

where

$$U_1 = \exp(i\theta_{14}\sigma_2), \quad (67)$$

and  $\sigma_2$  is one of the three Pauli matrices

$$\sigma_1 = \begin{pmatrix} 0 & 1 \\ 1 & 0 \end{pmatrix}, \quad \sigma_2 = \begin{pmatrix} 0 & -i \\ i & 0 \end{pmatrix}, \quad \sigma_3 = \begin{pmatrix} 1 & 0 \\ 0 & -1 \end{pmatrix}. \quad (68)$$

We denote the Hamiltonian of Eq. (66) as  $H_1$  and rewrite it as follows:

$$\begin{aligned} H_1 &= \exp(i\theta_{14}\sigma_2) \frac{\Delta E}{2} (\mathbf{1}_2 - \sigma_3) \exp(-i\theta_{14}\sigma_2) + \frac{A_e}{2} (\mathbf{1}_2 + \sigma_3) + \frac{A_s}{2} (\mathbf{1}_2 - \sigma_3) \\ &= \frac{\Delta E + A_e + A_s}{2} \mathbf{1}_2 - \frac{1}{2} (\alpha \sigma_3 - \beta \sigma_1), \end{aligned} \quad (69)$$

where

$$\alpha = \Delta E \cos 2\theta_{14} - A_e + A_s, \quad \beta = \Delta E \sin 2\theta_{14}, \quad (70)$$

and  $\mathbf{1}_2$  is the  $2 \times 2$  identity matrix. Denoting the mixing angle in matter as  $\tilde{\theta}_{14}$ , we have

$$\begin{aligned} &\exp(-i\tilde{\theta}_{14}\sigma_2) (\alpha \sigma_3 - \beta \sigma_1) \exp(i\tilde{\theta}_{14}\sigma_2) \\ &= (\alpha \cos 2\tilde{\theta}_{14} + \beta \sin 2\tilde{\theta}_{14}) \sigma_3 + (\alpha \sin 2\tilde{\theta}_{14} - \beta \cos 2\tilde{\theta}_{14}) \sigma_1. \end{aligned} \quad (71)$$

If we define

$$\tan 2\tilde{\theta}_{14} = \frac{\beta}{\alpha} = \frac{\Delta E \sin 2\theta_{14}}{\Delta E \cos 2\theta_{14} - A_e + A_s}, \quad (72)$$

which implies

$$\sin 2\tilde{\theta}_{14} = \frac{\beta}{\sqrt{\alpha^2 + \beta^2}}, \quad \cos 2\tilde{\theta}_{14} = \frac{\alpha}{\sqrt{\alpha^2 + \beta^2}}, \quad (73)$$

we obtain

$$\alpha\sigma_3 - \beta\sigma_1 = \sqrt{\alpha^2 + \beta^2} \exp(i\tilde{\theta}_{14}\sigma_2)\sigma_3 \exp(-i\tilde{\theta}_{14}\sigma_2). \quad (74)$$

Further, if we define

$$\Delta\tilde{E}_1 = \sqrt{\alpha^2 + \beta^2} = \sqrt{(\Delta E \cos 2\theta_{14} - A_e + A_s)^2 + (\Delta E \sin 2\theta_{14})^2}, \quad (75)$$

Eq. (69) becomes

$$\begin{aligned} H_1 &= \exp(i\tilde{\theta}_{14}\sigma_2) \left( \frac{\Delta E + A_e + A_s}{2} \mathbf{1}_2 - \frac{1}{2} \Delta\tilde{E}_1 \sigma_3 \right) \exp(-i\tilde{\theta}_{14}\sigma_2) \\ &= \exp(i\tilde{\theta}_{14}\sigma_2) \begin{pmatrix} \varepsilon_{1-} & 0 \\ 0 & \varepsilon_{1+} \end{pmatrix} \exp(-i\tilde{\theta}_{14}\sigma_2), \end{aligned} \quad (76)$$

where

$$\varepsilon_{1\mp} = \frac{\Delta E + A_e + A_s}{2} \mp \frac{1}{2} \Delta\tilde{E}_1. \quad (77)$$

From these discussions, the oscillation probability in this case is obtained by replacing  $\theta_{14}$  by  $\tilde{\theta}_{14}$  and  $\Delta E$  by  $\Delta\tilde{E}_1$  in the vacuum oscillation probability, and we obtain Eq. (29).

## B Derivation of Eqs. (37) and (38) in the case of $\theta_{14} = 0$ , $\theta_{24} \neq 0$ , and $\theta_{34} \neq 0$

In this Appendix, we discuss oscillations of atmospheric neutrinos for  $\theta_{14} = 0$ ,  $\theta_{24} \neq 0$ , and  $\theta_{34} \neq 0$ . In this case, it turns out that resonance occurs in the antineutrino mode. So, we start with Eq. (16) for antineutrinos. There is mixing among  $\bar{\nu}_\mu$ ,  $\bar{\nu}_\tau$  and  $\bar{\nu}_s$ , and Eq. (16) reduces to that in the three-flavor case

$$i \frac{d}{dt} \begin{pmatrix} \bar{\nu}_\mu \\ \bar{\nu}_\tau \\ \bar{\nu}_s \end{pmatrix} = \left[ U_2^* \begin{pmatrix} 0 & 0 & 0 \\ 0 & 0 & 0 \\ 0 & 0 & \Delta E \end{pmatrix} U_2^{*-1} + \begin{pmatrix} 0 & 0 & 0 \\ 0 & 0 & 0 \\ 0 & 0 & -A_s \end{pmatrix} \right] \begin{pmatrix} \bar{\nu}_\mu \\ \bar{\nu}_\tau \\ \bar{\nu}_s \end{pmatrix}. \quad (78)$$

In the discussions of the three-flavor mixing case, it is useful to introduce the following three Gell-Mann matrices:

$$\lambda_2 = \begin{pmatrix} 0 & -i & 0 \\ i & 0 & 0 \\ 0 & 0 & 0 \end{pmatrix}, \quad \lambda_5 = \begin{pmatrix} 0 & 0 & -i \\ 0 & 0 & 0 \\ i & 0 & 0 \end{pmatrix}, \quad \lambda_7 = \begin{pmatrix} 0 & 0 & 0 \\ 0 & 0 & -i \\ 0 & i & 0 \end{pmatrix}. \quad (79)$$

Now using the property of  $3 \times 3$  matrices

$$\begin{aligned} \text{diag}(1, e^{-i\delta_3/2}, e^{i\delta_3/2}) &= \text{diag}(1, e^{i\delta_3/2}, e^{i\delta_3/2}) \cdot \text{diag}(1, e^{-i\delta_3}, 1), \\ \exp(i\theta_{34}\lambda_7) \cdot \text{diag}(1, e^{i\delta_3/2}, e^{i\delta_3/2}) &= \text{diag}(1, e^{i\delta_3/2}, e^{i\delta_3/2}) \cdot \exp(i\theta_{34}\lambda_7), \\ \text{diag}(1, e^{-i\delta_3}, 1) \cdot \exp(i\theta_{24}\lambda_5) &= \exp(i\theta_{24}\lambda_5) \cdot \text{diag}(1, e^{-i\delta_3}, 1), \end{aligned}$$

in the limit of one mass scale dominance, we can show that the diagonal matrix  $\text{diag}(1, e^{i\delta_3/2}, e^{i\delta_3/2})$  ( $\text{diag}(1, e^{-i\delta_3}, 1)$ ) with a CP phase  $\delta_3$  can be moved to the left of  $\exp(i\theta_{34}\lambda_7)$  (the right of  $\exp(i\theta_{24}\lambda_5)$ ), respectively:

$$\begin{aligned} U_2^* &= \text{diag}(1, e^{i\delta_3/2}, e^{-i\delta_3/2}) \cdot \exp(i\theta_{34}\lambda_7) \cdot \text{diag}(1, e^{-i\delta_3/2}, e^{i\delta_3/2}) \cdot \exp(i\theta_{24}\lambda_5) \\ &= \text{diag}(1, e^{i\delta_3/2}, e^{-i\delta_3/2}) \cdot \text{diag}(1, e^{i\delta_3/2}, e^{i\delta_3/2}) \cdot \exp(i\theta_{34}\lambda_7) \\ &\quad \times \exp(i\theta_{24}\lambda_5) \cdot \text{diag}(1, e^{-i\delta_3}, 1) \\ &= \text{diag}(1, e^{i\delta_3}, 1) \cdot \exp(i\theta_{34}\lambda_7) \cdot \exp(i\theta_{24}\lambda_5) \cdot \text{diag}(1, e^{-i\delta_3}, 1). \end{aligned} \quad (80)$$

The phase factor  $\text{diag}(1, e^{-i\delta_3}, 1)$  cancels in  $U_2^* \text{diag}(0, 0, \Delta E) U_2^{*-1}$ , and by redefining  $(\bar{\nu}_\mu, \bar{\nu}_\tau, \bar{\nu}_s)^T$  by  $\text{diag}(1, e^{-i\delta_3}, 1)(\bar{\nu}_\mu, \bar{\nu}_\tau, \bar{\nu}_s)^T$ , the CP phase  $\delta_3$  disappears in the one mass scale dominance limit. Therefore, in the following discussions, we set  $\delta_3 = 0$  for simplicity. In this case, there is no difference between  $U_2$  and  $U_2^*$ , so we denote  $U_2^*$  as  $U_2$  for simplicity in the following discussions. To transform Eq. (78) into a more familiar form, we introduce the following matrix

$$R = \begin{pmatrix} 0 & 0 & 1 \\ 0 & 1 & 0 \\ 1 & 0 & 0 \end{pmatrix} \quad (R^2 = \mathbf{1}_3), \quad (81)$$

where  $\mathbf{1}_3$  is the  $3 \times 3$  identity matrix. Then the Hamiltonian  $H_2$  on the right hand side of Eq. (78) can be transformed into

$$H_2 = R \left[ RU_2 \begin{pmatrix} 0 & 0 & 0 \\ 0 & 0 & 0 \\ 0 & 0 & \Delta E \end{pmatrix} U_2^{-1} R + \begin{pmatrix} -A_s & 0 & 0 \\ 0 & 0 & 0 \\ 0 & 0 & 0 \end{pmatrix} \right] R. \quad (82)$$

Next we define

$$H_2' = RU_2 \begin{pmatrix} 0 & 0 & 0 \\ 0 & 0 & 0 \\ 0 & 0 & \Delta E \end{pmatrix} U_2^{-1} R + \begin{pmatrix} -A_s & 0 & 0 \\ 0 & 0 & 0 \\ 0 & 0 & 0 \end{pmatrix}, \quad (83)$$

and find that  $H_2'$  is similar to the Hamiltonian of the evolution equation of flavor eigenstates of neutrinos in the standard three-flavor framework including the matter effect, when  $\Delta E_{21} = \Delta m_{21}^2/(2E)$  vanishes. Therefore, in comparison with the standard PMNS matrix (the CP phase is defined as  $\eta$ ), which is marked as  $U_{PMNS}$  in the following, we have

$$RU_2 = U_{PMNS} = \exp(i\varphi_{23}\lambda_7) \cdot \Gamma(\eta) \cdot \exp(i\varphi_{13}\lambda_5) \cdot \Gamma(\eta)^{-1} \cdot \exp(i\varphi_{12}\lambda_2), \quad (84)$$

where

$$\Gamma(\eta) = \text{diag}(e^{-i\eta/2}, 0, e^{i\eta/2}). \quad (85)$$

Note that we have used  $\varphi_{23}$ ,  $\varphi_{13}$  and  $\varphi_{12}$  to avoid confusion with the original mixing angles  $\theta_{23}$ ,  $\theta_{13}$ , and  $\theta_{12}$  in the  $4 \times 4$  matrix  $U$  in Eq. (13). To make the sign of the first row consistent with the standard representation  $U_{PMNS}$ , we have to introduce

a phase matrix, and we have

$$\begin{aligned}
RU_2 &= \begin{pmatrix} -s_{24}c_{34} & -s_{34} & c_{24}c_{34} \\ -s_{24}s_{34} & c_{34} & c_{24}s_{34} \\ c_{24} & 0 & s_{24} \end{pmatrix} \\
&= \text{diag}(-1, 1, 1) \cdot U_{PMNS} \\
&= \begin{pmatrix} -C_{12}C_{13} & -S_{12}C_{13} & -e^{-i\eta}S_{13} \\ -S_{12}C_{23} - e^{i\eta}C_{12}S_{13}S_{23} & C_{12}C_{23} - e^{i\eta}S_{12}S_{13}S_{23} & C_{13}S_{23} \\ S_{12}S_{23} - e^{i\eta}C_{12}S_{13}C_{23} & -C_{12}S_{23} - e^{i\eta}S_{12}S_{13}C_{23} & C_{13}C_{23} \end{pmatrix}, \quad (86)
\end{aligned}$$

where  $\text{diag}(-1, 1, 1)$  is a diagonal matrix with a phase that does not affect the oscillation probability, and we have defined  $s_{ij} = \sin \theta_{ij}$ ,  $c_{ij} = \cos \theta_{ij}$ ,  $S_{ij} = \sin \varphi_{ij}$  and  $C_{ij} = \cos \varphi_{ij}$ . From Eq. (86), we observe that the CP phase must satisfy  $\eta = \pi$  for variables  $S_{ij}$  and  $C_{ij}$ , which are semipositive definite, to satisfy  $[RU_2]_{32} = -C_{12}S_{23} - e^{i\eta}S_{12}S_{13}C_{23} = 0$ . In this case, we have

$$\tan \varphi_{12} = \frac{\tan \varphi_{23}}{S_{13}}; \quad (87)$$

from this we can derive the following three components of  $U_{PMNS}$ :

$$\begin{aligned}
[RU_2]_{21} &= -S_{12}C_{23} - e^{i\eta}C_{12}S_{13}S_{23} \\
&= -S_{12}C_{23} + C_{12}S_{13}S_{23} \\
&= C_{12}(-C_{23}\tan \varphi_{12} + S_{13}S_{23}) \\
&= C_{12}\left(-C_{23}\frac{\tan \varphi_{23}}{S_{13}} + S_{13}S_{23}\right) \\
&= -\frac{C_{12}S_{23}C_{13}^2}{S_{13}} < 0, \quad (88)
\end{aligned}$$

$$\begin{aligned}
[RU_2]_{22} &= C_{12}C_{23} - e^{i\eta}S_{12}S_{13}S_{23} \\
&= C_{12}C_{23} + S_{12}S_{13}S_{23} \\
&= C_{12}(C_{23} + S_{13}S_{23}\tan \varphi_{12}) \\
&= C_{12}\left(C_{23} + S_{13}S_{23}\frac{\tan \varphi_{23}}{S_{13}}\right) \\
&= \frac{C_{12}}{C_{23}}(C_{23}^2 + S_{23}^2) = \frac{C_{12}}{C_{23}} > 0, \quad (89)
\end{aligned}$$

$$\begin{aligned}
[RU_2]_{31} &= S_{12}S_{23} - e^{i\eta}C_{12}S_{13}C_{23} \\
&= S_{12}S_{23} + C_{12}S_{13}C_{23} \\
&= C_{12}(S_{23}\tan \varphi_{12} + S_{13}C_{23}) \\
&= C_{12}\left(S_{23}\frac{\tan \varphi_{23}}{S_{13}} + S_{13}C_{23}\right) \\
&= \frac{C_{12}}{C_{23}S_{13}}(S_{23}^2 + S_{13}^2C_{23}^2) > 0, \quad (90)
\end{aligned}$$

and obtain

$$\begin{aligned} & \text{diag}(-1, 1, 1) \cdot U_{PMNS} \\ &= \begin{pmatrix} -C_{12}C_{13} & -S_{12}C_{13} & S_{13} \\ -\frac{C_{12}S_{23}C_{13}^2}{S_{13}} & \frac{C_{12}}{C_{23}} & C_{13}S_{23} \\ \frac{C_{12}}{C_{23}S_{13}}(S_{23}^2 + S_{13}^2C_{23}^2) & 0 & C_{13}C_{23} \end{pmatrix}. \end{aligned} \quad (91)$$

From Eqs. (86) and (91) we obtain

$$\tan \varphi_{12} = \frac{t_{34}}{s_{24}} \quad (34)$$

$$\sin \varphi_{13} = c_{24}c_{34} \quad (35)$$

$$\tan \varphi_{23} = \frac{s_{34}}{t_{24}}, \quad (36)$$

where  $t_{ij} = \tan \theta_{ij}$  ( $i, j = 1, \dots, 4$ ). Eqs. (34), (35), (36) are consistent with all elements of  $RU_2$  in Eq. (86) for the region  $0 \leq \theta_{i4} \leq \pi/2$  ( $i = 2, 3$ ),  $0 \leq \varphi_{ij} \leq \pi/2$  ( $i, j = 1, 2, 3$ ). Based on Eqs. (82), (83) and (84), we can rewrite the Hamiltonian  $H_2$  as follows:

$$\begin{aligned} H_2 &= R \exp(i\varphi_{23}\lambda_7) \\ &\times \left[ \exp(i\varphi_{13}\lambda_5) \begin{pmatrix} 0 & 0 & 0 \\ 0 & 0 & 0 \\ 0 & 0 & \Delta E \end{pmatrix} \exp(-i\varphi_{13}\lambda_5) + \begin{pmatrix} -A_s & 0 & 0 \\ 0 & 0 & 0 \\ 0 & 0 & 0 \end{pmatrix} \right] \\ &\times \exp(-i\varphi_{23}\lambda_7) R. \end{aligned} \quad (92)$$

Similarly to the case in Subsubsection 3.1.1, we have

$$\begin{aligned} H_2 &= R \exp(i\varphi_{23}\lambda_7) \exp(i\tilde{\varphi}_{13}\lambda_5) \\ &\times \begin{pmatrix} \varepsilon_{2-} & 0 & 0 \\ 0 & 0 & 0 \\ 0 & 0 & \varepsilon_{2+} \end{pmatrix} \\ &\times \exp(-i\tilde{\varphi}_{13}\lambda_5) \exp(-i\varphi_{23}\lambda_7) R. \end{aligned} \quad (93)$$

where

$$\tan 2\tilde{\varphi}_{13} = \frac{\Delta E \sin 2\varphi_{13}}{\Delta E \cos 2\varphi_{13} + A_s}, \quad (39)$$

$$\varepsilon_{2\mp} = \frac{\Delta E - A_s}{2} \mp \frac{1}{2} \Delta \tilde{E}_2, \quad (40)$$

and

$$\Delta \tilde{E}_2 = \sqrt{(\Delta E \cos 2\varphi_{13} + A_s)^2 + (\Delta E \sin 2\varphi_{13})^2}. \quad (41)$$

Since the mixing between active and sterile neutrinos are expected to be very weak in the (3+1)-scheme, we can consider

$$|\theta_{24}| \ll 1, \quad |\theta_{34}| \ll 1. \quad (94)$$



Then, from (35) we obtain

$$\varphi_{13} \simeq \frac{\pi}{2}. \quad (95)$$

Thus, Eq. (39) becomes

$$\tan 2\tilde{\varphi}_{13} \simeq \frac{\Delta E \sin 2\varphi_{13}}{-\Delta E + A_s}. \quad (96)$$

Eq. (96) indicates that there is resonance in the disappearance channel  $\bar{\nu}_\mu \rightarrow \bar{\nu}_\mu$  and the appearance channel  $\bar{\nu}_\mu \rightarrow \bar{\nu}_\tau$ . From these, the oscillation probabilities  $P(\bar{\nu}_\mu \rightarrow \bar{\nu}_\mu)$  and  $P(\bar{\nu}_\mu \rightarrow \bar{\nu}_\tau)$  can be, respectively, expressed as follows:

$$P(\bar{\nu}_\mu \rightarrow \bar{\nu}_\mu) = 1 - C_{23}^4 \sin^2 2\tilde{\varphi}_{13} \sin^2 \left( \frac{\Delta \tilde{E}_2 L}{2} \right) - \sin^2 2\varphi_{23} \left\{ \tilde{S}_{13}^2 \sin^2 \left( \frac{\varepsilon_{2-L}}{2} \right) + \tilde{C}_{13}^2 \sin^2 \left( \frac{\varepsilon_{2+L}}{2} \right) \right\}, \quad (37)$$

$$P(\bar{\nu}_\mu \rightarrow \bar{\nu}_\tau) = \sin^2 2\varphi_{23} \left\{ \tilde{S}_{13}^2 \sin^2 \left( \frac{\varepsilon_{2-L}}{2} \right) + \tilde{C}_{13}^2 \sin^2 \left( \frac{\varepsilon_{2+L}}{2} \right) - \frac{1}{4} \sin^2 2\tilde{\varphi}_{13} \sin^2 \left( \frac{\Delta \tilde{E}_2 L}{2} \right) \right\}, \quad (38)$$

## C Derivation of Eq. (48) in the case of $\theta_{14} \neq 0$ , and $\theta_{24} = \theta_{34} = 0$

In this Appendix, we discuss oscillations of astrophysical neutrinos for  $\theta_{14} \neq 0$ , and  $\theta_{24} = \theta_{34} = 0$ . As in the discussion in Subsubsection 3.1.1, we consider the case of the neutrino mode. Based on Eq. (76) in Subsubsection 3.1.1, it is not difficult to explicitly obtain the transition matrix  $T$ :

$$T = \exp(i\tilde{\theta}_{14}\mathcal{T}_{14}) \cdot \begin{pmatrix} e^{-iL\varepsilon_{1-}} & 0 & 0 & 0 \\ 0 & 1 & 0 & 0 \\ 0 & 0 & 1 & 0 \\ 0 & 0 & 0 & e^{-iL\varepsilon_{1+}} \end{pmatrix} \cdot \exp(-i\tilde{\theta}_{14}\mathcal{T}_{14}) \\ = \begin{pmatrix} \tilde{c}_{14}^2 e^{-iL\varepsilon_{1-}} + \tilde{s}_{14}^2 e^{-iL\varepsilon_{1+}} & 0 & 0 & \tilde{s}_{14}\tilde{c}_{14} (e^{-iL\varepsilon_{1+}} - e^{-iL\varepsilon_{1-}}) \\ 0 & 1 & 0 & 0 \\ 0 & 0 & 1 & 0 \\ \tilde{s}_{14}\tilde{c}_{14} (e^{-iL\varepsilon_{1+}} - e^{-iL\varepsilon_{1-}}) & 0 & 0 & \tilde{s}_{14}^2 e^{-iL\varepsilon_{1-}} + \tilde{c}_{14}^2 e^{-iL\varepsilon_{1+}} \end{pmatrix}, \quad (97)$$

where

$$\mathcal{T}_{14} = \begin{pmatrix} 0 & 0 & 0 & -i \\ 0 & 0 & 0 & 0 \\ 0 & 0 & 0 & 0 \\ i & 0 & 0 & 0 \end{pmatrix}. \quad (98)$$

Here, we can write down the non-zero matrix elements of  $T$ :<sup>5</sup>

$$\begin{aligned}
T_{11} &= \tilde{c}_{14}^2 e^{-iL\varepsilon_{1-}} + \tilde{s}_{14}^2 e^{-iL\varepsilon_{1+}}, \\
T_{14} &= T_{41} = \tilde{s}_{14}\tilde{c}_{14} (e^{-iL\varepsilon_{1+}} - e^{-iL\varepsilon_{1-}}), \\
T_{22} &= T_{33} = 1, \\
T_{44} &= \tilde{s}_{14}^2 e^{-iL\varepsilon_{1-}} + \tilde{c}_{14}^2 e^{-iL\varepsilon_{1+}},
\end{aligned} \tag{99}$$

where  $\tilde{s}_{14} = \sin \tilde{\theta}_{14}$ ,  $\tilde{c}_{14} = \cos \tilde{\theta}_{14}$  and  $\varepsilon_{1\mp}$  is given by Eq. (77). From Eq. (99) we have the following:

$$|T_{11}|^2 = 1 - \sin^2 2\tilde{\theta}_{14} \sin^2 \left( \frac{\Delta \tilde{E}_1 L}{2} \right) \tag{100}$$

$$|T_{14}|^2 = \sin^2 2\tilde{\theta}_{14} \sin^2 \left( \frac{\Delta \tilde{E}_1 L}{2} \right) \tag{49}$$

$$|T_{41}|^2 = \sin^2 2\tilde{\theta}_{14} \sin^2 \left( \frac{\Delta \tilde{E}_1 L}{2} \right) \tag{101}$$

$$|T_{44}|^2 = 1 - \sin^2 2\tilde{\theta}_{14} \sin^2 \left( \frac{\Delta \tilde{E}_1 L}{2} \right) \tag{102}$$

For later purposes, we keep the dependence of  $U$  on  $\theta_{14}$  but we use the following approximation for the three-flavor mixing angles in  $U$ :

$$\theta_{13} \simeq 0. \tag{103}$$

We introduce the product of matrices  $T$  and  $U$ :

$$\begin{aligned}
V &\equiv TU \\
&\simeq \begin{pmatrix} T_{11} & T_{12} & T_{13} & T_{14} \\ T_{21} & T_{22} & T_{23} & T_{24} \\ T_{31} & T_{32} & T_{33} & T_{34} \\ T_{41} & T_{42} & T_{43} & T_{44} \end{pmatrix} \begin{pmatrix} c_{14} & 0 & 0 & s_{14} \\ 0 & 1 & 0 & 0 \\ 0 & 0 & 1 & 0 \\ -s_{14} & 0 & 0 & c_{14} \end{pmatrix} \\
&\times \begin{pmatrix} c_{12} & s_{12} & 0 & 0 \\ -s_{12}c_{23} & c_{12}c_{23} & s_{23} & 0 \\ s_{12}s_{23} & -c_{12}s_{23} & c_{23} & 0 \\ 0 & 0 & 0 & 1 \end{pmatrix} \tag{104}
\end{aligned}$$

$$= \begin{pmatrix} c_{12}T_{1-} & s_{12}T_{1-} & 0 & T_{1+} \\ -s_{12}c_{23} & c_{12}c_{23} & s_{23} & 0 \\ s_{12}s_{23} & -c_{12}s_{23} & c_{23} & 0 \\ c_{12}T_{4-} & s_{12}T_{4-} & 0 & T_{4+} \end{pmatrix} \tag{105}$$

---

<sup>5</sup>The two indices of  $T$  and one of the indices of  $U$  must be that of flavor  $\alpha = e, \mu, \tau, s$ . For simplicity, we denote  $T_{ij}$  ( $i, j = 1, \dots, 4$ ) and  $U_{ij}$  ( $i, j = 1, \dots, 4$ ) instead of  $T_{\alpha\beta}$  ( $\alpha, \beta = e, \mu, \tau, s$ ) and  $U_{\alpha i}$  ( $\alpha = e, \mu, \tau, s; i = 1, \dots, 4$ ) in this appendix.

where

$$T_{1-} \equiv c_{14} T_{11} - s_{14} T_{14} \quad (106)$$

$$T_{1+} \equiv s_{14} T_{11} + c_{14} T_{14} \quad (107)$$

$$T_{4-} \equiv c_{14} T_{41} - s_{14} T_{44} \quad (108)$$

$$T_{4+} \equiv s_{14} T_{41} + c_{14} T_{44} \quad (109)$$

Then, from Eq. (47), we obtain the formulae of the oscillation probabilities:

$$\begin{aligned} & P(\nu_\alpha \rightarrow \nu_\beta) \\ &= \sum_i |V_{\beta i}|^2 |U_{\alpha i}|^2 \\ &\simeq \left[ \begin{pmatrix} c_{12}^2 |T_{1-}|^2 & s_{12}^2 |T_{1-}|^2 & 0 & |T_{1+}|^2 \\ s_{12}^2 c_{23}^2 & c_{12}^2 c_{23}^2 & s_{23}^2 & 0 \\ s_{12}^2 s_{23}^2 & c_{12}^2 s_{23}^2 & c_{23}^2 & 0 \\ c_{12}^2 |T_{4-}|^2 & s_{12}^2 |T_{4-}|^2 & 0 & |T_{4+}|^2 \end{pmatrix} \begin{pmatrix} c_{12}^2 c_{14}^2 & s_{12}^2 c_{23}^2 & s_{12}^2 s_{23}^2 & c_{12}^2 s_{14}^2 \\ s_{12}^2 c_{14}^2 & c_{12}^2 c_{23}^2 & c_{12}^2 s_{23}^2 & s_{12}^2 s_{14}^2 \\ 0 & s_{23}^2 & c_{23}^2 & 0 \\ s_{14}^2 & 0 & 0 & c_{14}^2 \end{pmatrix} \right]_{\beta\alpha}. \end{aligned} \quad (110)$$

Each probability is as follows:

$$P(\nu_e \rightarrow \nu_e) = c_{14}^2 (s_{12}^4 + c_{12}^4) |T_{1-}|^2 + s_{14}^2 |T_{1+}|^2, \quad (111)$$

$$P(\nu_e \rightarrow \nu_\mu) = 2c_{14}^2 s_{12}^2 c_{12}^2 c_{23}^2, \quad (112)$$

$$P(\nu_e \rightarrow \nu_\tau) = 2c_{14}^2 s_{12}^2 c_{12}^2 s_{23}^2, \quad (113)$$

$$P(\nu_e \rightarrow \nu_s) = c_{14}^2 (s_{12}^4 + c_{12}^4) |T_{4-}|^2 + s_{14}^2 |T_{4+}|^2; \quad (114)$$

and

$$P(\nu_\mu \rightarrow \nu_e) = 2s_{12}^2 c_{12}^2 c_{23}^2 |T_{1-}|^2, \quad (115)$$

$$P(\nu_\mu \rightarrow \nu_\mu) = (s_{12}^4 + c_{12}^4) c_{23}^4 + s_{23}^4, \quad (116)$$

$$P(\nu_\mu \rightarrow \nu_\tau) = (s_{12}^4 + c_{12}^4 + 1) s_{23}^2 c_{23}^2, \quad (117)$$

$$P(\nu_\mu \rightarrow \nu_s) = 2s_{12}^2 c_{12}^2 c_{23}^2 |T_{4-}|^2. \quad (118)$$

It is known that at the production source of astrophysical neutrinos, such as active galactic nuclei, the ratios of the flux of  $\nu_e$ ,  $\nu_\mu$  and  $\nu_\tau$  is 1:2:0. Moreover, it is expected that there is no sterile neutrino at the source. Denoting the flux of astrophysical neutrinos at the source as  $F^0(\nu_\alpha)$  ( $\alpha = e, \mu, \tau, s$ ), we have  $F^0(\nu_e) : F^0(\nu_\mu) : F^0(\nu_\tau) : F^0(\nu_s) = 1 : 2 : 0 : 0$ . From Eq. (4), to a good approximation, we can assume that  $\theta_{23} \simeq \pi/4$ , so that  $s_{23} \simeq c_{23} \simeq 1/\sqrt{2}$ . Thus we can estimate the flux of  $\nu_e$ ,  $\nu_\mu$ ,  $\nu_\tau$  and  $\nu_s$ , which is observed at IceCube is given in the unit of  $F^0(\nu_e)$

by:

$$\begin{aligned} F(\nu_e) &= P(\nu_e \rightarrow \nu_e) + 2P(\nu_\mu \rightarrow \nu_e) \\ &\simeq \{c_{14}^2 (s_{12}^4 + c_{12}^4) + 2s_{12}^2 c_{12}^2\} |T_{1-}|^2 + s_{14}^2 |T_{1+}|^2, \end{aligned} \quad (119)$$

$$\begin{aligned} F(\nu_\mu) &= P(\nu_e \rightarrow \nu_\mu) + 2P(\nu_\mu \rightarrow \nu_\mu) \\ &\simeq c_{14}^2 s_{12}^2 c_{12}^2 + \frac{1}{2} (s_{12}^4 + c_{12}^4 + 1), \end{aligned} \quad (120)$$

$$\begin{aligned} F(\nu_\tau) &= P(\nu_e \rightarrow \nu_\tau) + 2P(\nu_\mu \rightarrow \nu_\tau) \\ &\simeq c_{14}^2 s_{12}^2 c_{12}^2 + \frac{1}{2} (s_{12}^4 + c_{12}^4 + 1), \end{aligned} \quad (121)$$

$$\begin{aligned} F(\nu_s) &= P(\nu_e \rightarrow \nu_s) + 2P(\nu_\mu \rightarrow \nu_s) \\ &\simeq \{c_{14}^2 (s_{12}^4 + c_{12}^4) + 2s_{12}^2 c_{12}^2\} |T_{4-}|^2 + s_{14}^2 |T_{4+}|^2. \end{aligned} \quad (122)$$

If we use approximation  $\theta_{14} \simeq 0$  except in  $T_{i\pm}$  ( $i = 1, 4$ ) while keeping  $\tilde{\theta}_{14} \neq 0$  in each flux, from Eqs. (106), (108), (100) and (49), we have

$$|T_{1-}|^2 \simeq |T_{11}|^2 = 1 - \sin^2 2\tilde{\theta}_{14} \sin^2 \left( \frac{\Delta \tilde{E}_1 L}{2} \right) \quad (123)$$

$$|T_{4-}|^2 \simeq |T_{41}|^2 = \sin^2 2\tilde{\theta}_{14} \sin^2 \left( \frac{\Delta \tilde{E}_1 L}{2} \right) \quad (124)$$

Hence, the ratio of each flavor of neutrino can be approximated as

$$F(\nu_e) : F(\nu_\mu) : F(\nu_\tau) : F(\nu_s) \simeq 1 - |T_{14}|^2 : 1 : 1 : |T_{14}|^2, \quad (48)$$

where  $|T_{14}|^2$  is defined in Eq. (49) and  $|T_{14}|^2$  has nontrivial dependence on the neutrino energy  $E$ , especially near the resonance region  $E \sim \Delta m_{41}^2 / \{2(A_e - A_s)\}$ .

## D Derivation of Eq. (50) in the case of $\theta_{14} = 0$ , $\theta_{24} \neq 0$ , and $\theta_{34} \neq 0$

In this Appendix, we discuss oscillations of astrophysical neutrinos for  $\theta_{14} = 0$ ,  $\theta_{24} \neq 0$  and  $\theta_{34} \neq 0$ . As in Subsubsection 3.1.2, it is useful to discuss in terms of the new mixing angles in Eqs. (34), (35), (36). According to Eq. (93) in Subsubsection 3.1.2, we can explicitly express the transition matrix  $T$ :

$$T = \begin{pmatrix} e^{-iLA_e} & 0 & 0 & 0 \\ 0 & T_{22} & T_{23} & T_{24} \\ 0 & T_{32} & T_{33} & T_{34} \\ 0 & T_{42} & T_{43} & T_{44} \end{pmatrix}. \quad (125)$$

Here, we denote the submatrix of  $T$  by  $T_0$ :

$$\begin{aligned} T_0 &= \begin{pmatrix} T_{22} & T_{23} & T_{24} \\ T_{32} & T_{33} & T_{34} \\ T_{42} & T_{43} & T_{44} \end{pmatrix} \\ &= R e^{i\varphi_{23}\lambda_7} e^{i\tilde{\varphi}_{13}\lambda_5} \begin{pmatrix} e^{-iL\varepsilon_{2-}} & 0 & 0 \\ 0 & 1 & 0 \\ 0 & 0 & e^{-iL\varepsilon_{2+}} \end{pmatrix} e^{-i\tilde{\varphi}_{13}\lambda_5} e^{-i\varphi_{23}\lambda_7} R, \end{aligned} \quad (126)$$

where

$$\begin{aligned}
T_{22} &= \left( \tilde{S}_{13}^2 e^{-iL\varepsilon_{2-}} + \tilde{C}_{13}^2 e^{-iL\varepsilon_{2+}} \right) C_{23}^2 + S_{23}^2, \\
T_{23} &= T_{32} = \left( \tilde{S}_{13}^2 e^{-iL\varepsilon_{2-}} + \tilde{C}_{13}^2 e^{-iL\varepsilon_{2+}} - 1 \right) S_{23} C_{23}, \\
T_{24} &= T_{42} = \left( e^{-iL\varepsilon_{2+}} - e^{-iL\varepsilon_{2-}} \right) \tilde{S}_{13} \tilde{C}_{13} C_{23}, \\
T_{33} &= \left( \tilde{S}_{13}^2 e^{-iL\varepsilon_{2-}} + \tilde{C}_{13}^2 e^{-iL\varepsilon_{2+}} \right) S_{23}^2 + C_{23}^2, \\
T_{34} &= T_{43} = \left( e^{-iL\varepsilon_{2+}} - e^{-iL\varepsilon_{2-}} \right) \tilde{S}_{13} \tilde{C}_{13} S_{23}, \\
T_{44} &= \tilde{C}_{13}^2 e^{-iL\varepsilon_{2-}} + \tilde{S}_{13}^2 e^{-iL\varepsilon_{2+}}.
\end{aligned} \tag{127}$$

From Eqs. (127), we have the following:

$$\begin{aligned}
|T_{22}|^2 &= S_{23}^4 + C_{23}^4 \left\{ 1 - \sin^2 2\tilde{\varphi}_{13} \sin^2 \left( \frac{\Delta \tilde{E}_2 L}{2} \right) \right\} \\
&\quad + 2C_{23}^2 S_{23}^2 \operatorname{Re} \left[ e^{-i(\Delta E - A_s)L/2} \left\{ \cos \left( \frac{\Delta \tilde{E}_2 L}{2} \right) - i \cos 2\tilde{\varphi}_{13} \sin \left( \frac{\Delta \tilde{E}_2 L}{2} \right) \right\} \right],
\end{aligned} \tag{128}$$

$$\begin{aligned}
|T_{23}|^2 &= |T_{32}|^2 \\
&= C_{23}^2 S_{23}^2 \left\{ 2 - \sin^2 2\tilde{\varphi}_{13} \sin^2 \left( \frac{\Delta \tilde{E}_2 L}{2} \right) \right\} \\
&\quad - 2C_{23}^2 S_{23}^2 \operatorname{Re} \left[ e^{-i(\Delta E - A_s)L/2} \left\{ \cos \left( \frac{\Delta \tilde{E}_2 L}{2} \right) - i \cos 2\tilde{\varphi}_{13} \sin \left( \frac{\Delta \tilde{E}_2 L}{2} \right) \right\} \right],
\end{aligned} \tag{129}$$

$$\begin{aligned}
|T_{24}|^2 &= |T_{42}|^2 \\
&= C_{23}^2 \sin^2 2\tilde{\varphi}_{13} \sin^2 \left( \frac{\Delta \tilde{E}_2 L}{2} \right),
\end{aligned} \tag{130}$$

$$\begin{aligned}
|T_{33}|^2 &= C_{23}^4 + S_{23}^4 \left\{ 1 - \sin^2 2\tilde{\varphi}_{13} \sin^2 \left( \frac{\Delta \tilde{E}_2 L}{2} \right) \right\} \\
&\quad + 2C_{23}^2 S_{23}^2 \operatorname{Re} \left[ e^{-i(\Delta E - A_s)L/2} \left\{ \cos \left( \frac{\Delta \tilde{E}_2 L}{2} \right) - i \cos 2\tilde{\varphi}_{13} \sin \left( \frac{\Delta \tilde{E}_2 L}{2} \right) \right\} \right],
\end{aligned} \tag{131}$$

$$\begin{aligned}
|T_{34}|^2 &= |T_{43}|^2 \\
&= S_{23}^2 \sin^2 2\tilde{\varphi}_{13} \sin^2 \left( \frac{\Delta \tilde{E}_2 L}{2} \right),
\end{aligned} \tag{132}$$

$$|T_{44}|^2 = 1 - \sin^2 2\tilde{\varphi}_{13} \sin^2 \left( \frac{\Delta \tilde{E}_2 L}{2} \right). \tag{51}$$

Here, we have defined  $\tilde{S}_{13} = \sin \tilde{\varphi}_{13}$ ,  $\tilde{C}_{13} = \cos \tilde{\varphi}_{13}$ ,  $S_{23} = \sin \varphi_{23}$ ,  $C_{23} = \cos \varphi_{23}$  and  $\varepsilon_{2\mp}$  is given by Eq. (40).

Then, according to Eq. (47), using approximation  $\theta_{13} \simeq 0$ , we can obtain the formulae of oscillation probabilities:

$$P(\nu_e \rightarrow \nu_e) = 1 - 2s_{12}^2 c_{12}^2, \quad (133)$$

$$P(\nu_e \rightarrow \nu_\mu) = 2|T_{22}|^2 \cdot s_{12}^2 c_{12}^2 c_{23}^2 - 4\text{Re}(T_{22}T_{23}^*) \cdot s_{12}^2 c_{12}^2 s_{23} c_{23} + 2|T_{23}|^2 \cdot s_{12}^2 c_{12}^2 s_{23}^2, \quad (134)$$

$$P(\nu_e \rightarrow \nu_\tau) = 2|T_{32}|^2 \cdot s_{12}^2 c_{12}^2 c_{23}^2 - 4\text{Re}(T_{32}T_{33}^*) \cdot s_{12}^2 c_{12}^2 s_{23} c_{23} + 2|T_{33}|^2 \cdot s_{12}^2 c_{12}^2 s_{23}^2, \quad (135)$$

$$P(\nu_e \rightarrow \nu_s) = 2|T_{42}|^2 \cdot s_{12}^2 c_{12}^2 c_{23}^2 - 4\text{Re}(T_{42}T_{43}^*) \cdot s_{12}^2 c_{12}^2 s_{23} c_{23} + 2|T_{43}|^2 \cdot s_{12}^2 c_{12}^2 s_{23}^2; \quad (136)$$

and

$$P(\nu_\mu \rightarrow \nu_e) = 2s_{12}^2 c_{12}^2 c_{23}^2, \quad (137)$$

$$P(\nu_\mu \rightarrow \nu_\mu) = |T_{22}|^2 \cdot [(s_{12}^4 + c_{12}^4) c_{23}^4 + s_{23}^4] - 2\text{Re}(T_{22}T_{23}^*) \cdot [(s_{12}^4 + c_{12}^4) s_{23} c_{23}^3 - s_{23}^3 c_{23}] + |T_{23}|^2 \cdot [(s_{12}^4 + c_{12}^4) s_{23}^2 c_{23}^2 + s_{23}^2 c_{23}^2], \quad (138)$$

$$P(\nu_\mu \rightarrow \nu_\tau) = |T_{32}|^2 \cdot [(s_{12}^4 + c_{12}^4) c_{23}^4 + s_{23}^4] - 2\text{Re}(T_{32}T_{33}^*) \cdot [(s_{12}^4 + c_{12}^4) s_{23} c_{23}^3 - s_{23}^3 c_{23}] + |T_{33}|^2 \cdot [(s_{12}^4 + c_{12}^4) s_{23}^2 c_{23}^2 + s_{23}^2 c_{23}^2], \quad (139)$$

$$P(\nu_\mu \rightarrow \nu_s) = |T_{42}|^2 \cdot [(s_{12}^4 + c_{12}^4) c_{23}^4 + s_{23}^4] - 2\text{Re}(T_{42}T_{43}^*) \cdot [(s_{12}^4 + c_{12}^4) s_{23} c_{23}^3 - s_{23}^3 c_{23}] + |T_{43}|^2 \cdot [(s_{12}^4 + c_{12}^4) s_{23}^2 c_{23}^2 + s_{23}^2 c_{23}^2]. \quad (140)$$

As in Subsubsection 3.2.1, using approximation  $\theta_{23} \simeq \pi/4$ , we obtain the flux of  $\nu_e$ ,

$\nu_\mu$  and  $\nu_s$  observed at IceCube:

$$\begin{aligned}
F(\nu_e) &= P(\nu_e \rightarrow \nu_e) + 2P(\nu_\mu \rightarrow \nu_e) \\
&\simeq s_{12}^4 + c_{12}^4 + 4s_{12}^2 c_{12}^2 c_{23}^2 \\
&\simeq 1,
\end{aligned} \tag{141}$$

$$\begin{aligned}
F(\nu_\mu) &= P(\nu_e \rightarrow \nu_\mu) + 2P(\nu_\mu \rightarrow \nu_\mu) \\
&\simeq |T_{22}|^2 \cdot [2s_{12}^2 c_{12}^2 c_{23}^2 + 2(s_{12}^4 + c_{12}^4) c_{23}^4 + 2s_{23}^4] \\
&\quad - 4\text{Re}(T_{22}T_{23}^*) \cdot [s_{12}^2 c_{12}^2 s_{23} c_{23} + (s_{12}^4 + c_{12}^4) s_{23} c_{23}^3 - s_{23}^3 c_{23}] \\
&\quad + |T_{23}|^2 \cdot [2s_{12}^2 c_{12}^2 s_{23}^2 + 2(s_{12}^4 + c_{12}^4) s_{23}^2 c_{23}^2 + 2s_{23}^2 c_{23}^2] \\
&\simeq |T_{22}|^2 + |T_{23}|^2,
\end{aligned} \tag{142}$$

$$\begin{aligned}
F(\nu_\tau) &= P(\nu_e \rightarrow \nu_\tau) + 2P(\nu_\mu \rightarrow \nu_\tau) \\
&\simeq |T_{32}|^2 \cdot [2s_{12}^2 c_{12}^2 c_{23}^2 + 2(s_{12}^4 + c_{12}^4) c_{23}^4 + 2s_{23}^4] \\
&\quad - 4\text{Re}(T_{32}T_{33}^*) \cdot [s_{12}^2 c_{12}^2 s_{23} c_{23} + (s_{12}^4 + c_{12}^4) s_{23} c_{23}^3 - s_{23}^3 c_{23}] \\
&\quad + |T_{33}|^2 \cdot [2s_{12}^2 c_{12}^2 s_{23}^2 + 2(s_{12}^4 + c_{12}^4) s_{23}^2 c_{23}^2 + 2s_{23}^2 c_{23}^2] \\
&\simeq |T_{32}|^2 + |T_{33}|^2,
\end{aligned} \tag{143}$$

$$\begin{aligned}
F(\nu_s) &= P(\nu_e \rightarrow \nu_s) + 2P(\nu_\mu \rightarrow \nu_s) \\
&\simeq |T_{42}|^2 \cdot [2s_{12}^2 c_{12}^2 c_{23}^2 + 2(s_{12}^4 + c_{12}^4) c_{23}^4 + 2s_{23}^4] \\
&\quad - 4\text{Re}(T_{42}T_{43}^*) \cdot [s_{12}^2 c_{12}^2 s_{23} c_{23} + (s_{12}^4 + c_{12}^4) s_{23} c_{23}^3 - s_{23}^3 c_{23}] \\
&\quad + |T_{43}|^2 \cdot [2s_{12}^2 c_{12}^2 s_{23}^2 + 2(s_{12}^4 + c_{12}^4) s_{23}^2 c_{23}^2 + 2s_{23}^2 c_{23}^2] \\
&\simeq |T_{42}|^2 + |T_{43}|^2.
\end{aligned} \tag{144}$$

Hence the flavor ratio is given by

$$\begin{aligned}
&F(\nu_e) : F(\nu_\mu) : F(\nu_\tau) : F(\nu_s) \\
&\simeq 1 : 1 - |T_{24}|^2 : 1 - |T_{34}|^2 : 1 - |T_{44}|^2 \\
&= 1 : 1 - C_{23}^2 (1 - |T_{44}|^2) : 1 - S_{23}^2 (1 - |T_{44}|^2) : 1 - |T_{44}|^2,
\end{aligned} \tag{50}$$

where  $|T_{44}|^2$  is defined in Eq. (51) and  $|T_{44}|^2$  has nontrivial dependence on the neutrino energy  $E$ , especially near the resonance region  $E \sim \Delta m_{41}^2 / (2A_s)$ .

## E The behavior of astrophysical $\nu_e$ as $\theta_{14} \rightarrow \pi/4$

If  $\theta_{14}$  is very close to  $\pi/4$  and  $|\Delta E| \ll |A_e - A_s|$ , from Eqs. (30) and (31), we obtain

$$\cos 2\tilde{\theta}_{14} = \frac{\Delta E \cos 2\theta_{14} - A_e + A_s}{\Delta \tilde{E}_1} \simeq -1, \tag{145}$$

which indicates

$$\tilde{\theta}_{14} \simeq \frac{\pi}{2}. \tag{146}$$

From Eq. (106), we obtain

$$T_{1-} \simeq \frac{1}{\sqrt{2}} (T_{11} - T_{14}) \tag{147}$$

We can now calculate the factor  $|T_{1-}|^2$  in Eq. (119) as  $\theta_{14} \rightarrow \pi/4$  as follows.

$$\begin{aligned}
|T_{1-}|^2 &\simeq \frac{1}{2} |T_{11} - T_{14}|^2 \\
&= \frac{1}{2} \{ |T_{11}|^2 + |T_{14}|^2 - 2 \operatorname{Re} (T_{11} T_{14}^*) \} \\
&\simeq \frac{1}{2}
\end{aligned} \tag{148}$$

where we used the following properties and Eqs. (100) and (49):

$$T_{11} = e^{-i(\Delta E + A_e + A_s)L/2} \left\{ \cos \left( \frac{\Delta \tilde{E}_1 L}{2} \right) + i \cos 2\tilde{\theta}_{14} \sin \left( \frac{\Delta \tilde{E}_1 L}{2} \right) \right\} \tag{149}$$

$$T_{14} = -i e^{-i(\Delta E + A_e + A_s)L/2} \sin 2\tilde{\theta}_{14} \sin \left( \frac{\Delta \tilde{E}_1 L}{2} \right) \simeq 0. \tag{150}$$

Eq. (148) implies that the oscillation probability of  $\nu_e$  flux is independent of the neutrino energy  $E$  and baseline length  $L$  in the Earth.

## References

- [1] P. A. Zyla *et al.* [Particle Data Group], PTEP **2020** (2020) no.8, 083C01 doi:10.1093/ptep/ptaa104
- [2] A. Aguilar-Arevalo *et al.* [LSND], Phys. Rev. D **64** (2001), 112007 doi:10.1103/PhysRevD.64.112007 [arXiv:hep-ex/0104049 [hep-ex]].
- [3] A. A. Aguilar-Arevalo *et al.* [MiniBooNE], Phys. Rev. Lett. **121** (2018) no.22, 221801 doi:10.1103/PhysRevLett.121.221801 [arXiv:1805.12028 [hep-ex]].
- [4] K. N. Abazajian, M. A. Acero, S. K. Agarwalla, A. A. Aguilar-Arevalo, C. H. Albright, S. Antusch, C. A. Argüelles, A. B. Balantekin, G. Barenboim and V. Barger, *et al.* [arXiv:1204.5379 [hep-ph]].
- [5] C. Giunti and M. Laveder, Phys. Rev. C **83** (2011), 065504 doi:10.1103/PhysRevC.83.065504 [arXiv:1006.3244 [hep-ph]].
- [6] G. Mention, M. Fechner, T. Lasserre, T. A. Mueller, D. Lhuillier, M. Cribier and A. Letourneau, Phys. Rev. D **83** (2011), 073006 doi:10.1103/PhysRevD.83.073006 [arXiv:1101.2755 [hep-ex]].
- [7] P. Huber, Phys. Rev. C **84** (2011), 024617 [erratum: Phys. Rev. C **85** (2012), 029901] doi:10.1103/PhysRevC.85.029901 [arXiv:1106.0687 [hep-ph]].
- [8] D. Adey *et al.* [Daya Bay], Phys. Rev. Lett. **123** (2019) no.11, 111801 doi:10.1103/PhysRevLett.123.111801 [arXiv:1904.07812 [hep-ex]].
- [9] A. C. Hayes, J. L. Friar, G. T. Garvey, G. Jungman and G. Jonkmans, Phys. Rev. Lett. **112** (2014), 202501 doi:10.1103/PhysRevLett.112.202501 [arXiv:1309.4146 [nucl-th]].



- [10] P. Adamson *et al.* [MINOS+ and Daya Bay], Phys. Rev. Lett. **125** (2020) no.7, 071801 doi:10.1103/PhysRevLett.125.071801 [arXiv:2002.00301 [hep-ex]].
- [11] A. Nicolaidis, G. Tsirigoti and J. Hansson, [arXiv:hep-ph/9904415 [hep-ph]].
- [12] O. Yasuda, doi:10.1142/9789812777003\_0017 [arXiv:hep-ph/0102166 [hep-ph]].
- [13] H. Nunokawa, O. L. G. Peres and R. Zukanovich Funchal, Phys. Lett. B **562** (2003), 279-290 doi:10.1016/S0370-2693(03)00603-8 [arXiv:hep-ph/0302039 [hep-ph]].
- [14] M. G. Aartsen *et al.* [IceCube], Phys. Rev. D **102** (2020) no.5, 052009 doi:10.1103/PhysRevD.102.052009 [arXiv:2005.12943 [hep-ex]].
- [15] M. Maltoni, T. Schwetz, M. A. Tortola and J. W. F. Valle, New J. Phys. **6** (2004), 122 doi:10.1088/1367-2630/6/1/122 [arXiv:hep-ph/0405172 [hep-ph]].
- [16] V. A. Naumov, Phys. Lett. B **529** (2002), 199-211 doi:10.1016/S0370-2693(02)01258-3 [arXiv:hep-ph/0112249 [hep-ph]].
- [17] M. G. Aartsen *et al.* [IceCube], Phys. Rev. D **91** (2015), 122004 doi:10.1103/PhysRevD.91.122004 [arXiv:1504.03753 [astro-ph.HE]].
- [18] G. L. Fogli, E. Lisi, A. Marrone and D. Montanino, Phys. Lett. B **425** (1998), 341-344 doi:10.1016/S0370-2693(98)00077-X [arXiv:hep-ph/9711421 [hep-ph]].
- [19] R. Foot, R. R. Volkas and O. Yasuda, Phys. Lett. B **433** (1998), 82-87 doi:10.1016/S0370-2693(98)00706-0 [arXiv:hep-ph/9802287 [hep-ph]].
- [20] J. G. Learned and S. Pakvasa, Astropart. Phys. **3** (1995), 267-274 doi:10.1016/0927-6505(94)00043-3 [arXiv:hep-ph/9405296 [hep-ph]].
- [21] R. Gandhi, C. Quigg, M. H. Reno and I. Sarcevic, Phys. Rev. D **58** (1998), 093009 doi:10.1103/PhysRevD.58.093009 [arXiv:hep-ph/9807264 [hep-ph]].
- [22] M. Honda, T. Kajita, K. Kasahara, S. Midorikawa and T. Sanuki, Phys. Rev. D **75** (2007), 043006 doi:10.1103/PhysRevD.75.043006 [arXiv:astro-ph/0611418 [astro-ph]].
- [23] D. Chirkin, [arXiv:hep-ph/0407078 [hep-ph]].